Advanced Fiber Materials (2023) 5:36–58
https://doi.org/10.1007/s42765-022-00215-x

REVIEW

Fiber-Based Materials for Aqueous Zinc Ion Batteries

Hao Jia[1,3] · Kaiyu Liu[1] · Yintung Lam[3] · Benjamin Tawiah[4] · John H. Xin[3] · Wenqi Nie[2] · Shou-xiang Jiang[3]

Received: 6 June 2022 / Accepted: 20 September 2022 / Published online: 6 October 2022
© Donghua University, Shanghai, China 2022, corrected publication 2022

Abstract

Neutral aqueous zinc ion batteries (ZIBs) have tremendous potential for grid-level energy storage and portable wearable devices. However, certain performance deficiencies of the components have limited the employment of ZIBs in practical applications. Recently, a range of pristine materials and their composites with fiber-based structures have been used to produce more efficient cathodes, anodes, current collectors, and separators for addressing the current challenges in ZIBs. Numerous functional materials can be manufactured into different fiber forms, which can be subsequently converted into various yarn structures, or interwoven into different 2D and 3D fabric-like constructions to attain various electrochemical performances and mechanical flexibility. In this review, we provide an overview of the concepts and principles of fiber-based materials for ZIBs, after which the application of various materials in fiber-based structures are discussed under different domains of ZIB components. Consequently, the current challenges of these materials, fabrication technologies and corresponding future development prospects are addressed.

Keywords Aqueous zinc ion batteries · Fiber-based materials · High-performance electrodes · Wearable batteries

Introduction

Despite lithium-ion batteries (LIBs) being the most successful commercial battery, their development for large-scale production is currently experiencing severe barriers due to high cost and safety concerns [1–3]. The organic electrolytes used in LIBs are mostly flammable, toxic, and cause serious pollution and endanger human health, thus necessitating strict battery manufacturing conditions [4–6]. Therefore, abundant research work has begun to focus on new battery candidates to partially replace the usage of LIBs [7]. Notably, aqueous zinc-ion batteries (ZIBs) are now emerging for grid-level energy storage and portable wearable devices owing to their high reliability, low toxicity, and high ionic conductivity efficiency of aqueous electrolytes [8–10]. In comparison with the lithium metal anode for LIBs as indicated in Table 1, the zinc (Zn) metal anode endows the batteries with higher ionic conductivity in aqueous electrolyte and higher volumetric capacity at a relatively lower cost [11–13]. Moreover, the neutral electrolyte generally causes less corrosion than the alkaline electrolyte, which enhances safety performance. All of these advantages make ZIB one of the most promising candidates in recent decades.

With the favorable prospects of ZIBs, substantial efforts have been given to their development and advancement [14, 15]. Nevertheless, some performance issues arising from the selection of materials and structures for fabricating ZIB components should also be highlighted for continuous improvement of the quality of ZIBs. An aqueous ZIB is generally composed of cathode, anode, electrolyte, and separator parts. For the cathode materials, researchers have extensively investigated active materials such as vanadium

Hao Jia, Kaiyu Liu, and Yintung Lam have contributed equally to this work.

✉ Hao Jia
jiahao@jiangnan.edu.cn

✉ Wenqi Nie
wenqinie@163.com

✉ Shou-xiang Jiang
kinor.j@polyu.edu.hk

1 Key Laboratory of Eco-Textiles, Ministry of Education, Jiangnan University, Wuxi 214122, People's Republic of China

2 School of Textile and Garment, Anhui Polytechnic University, Wuhu 241000, People's Republic of China

3 School of Fashion and Textiles, The Hong Kong Polytechnic University, Hong Kong 999077, People's Republic of China

4 Department of Industrial Art (Textile), Kwame Nkrumah University of Science and Technology, PMB, Kumasi, Ghana

Table 1 Comparison between the metal anode in LIBs and ZIBs

Element	Ionic radius [Å]	Standard potential versus (SHE)	Theoretical gravimetric capacity ($mAh{\cdot}g^{-1}$)	Theoretical volumetric capacity ($mAh{\cdot}cm^{-3}$)	Ionic conductivity ($S{\cdot}cm^{-1}$)	Cost of metal anode ($USD{\cdot}kg^{-1}$)
Li	0.76	−3.04	3860	2061	10^{-3}-10^{-2} (organic electrolytes)	19.2
Zn	0.75	−0.76	820	5855	10^{-1}-6 (aqueous electrolytes)	2.2

oxide (V_xO_y) [16–19], manganese oxide (Mn_xO_y) [20–22], Prussian blue analogs [23], and organic electrode materials [24–26] in recent years. However, the electrochemical and physical properties of these materials are still inadequate for high-performance applications. For example, the transition metal oxides suffer from inherent low conductivity, which results in unsatisfactory capability and cycling stability [27, 28]. The capacity of Prussian blue is restricted by severe release problems, especially at high operating voltages [29]. In addition, organic electrode materials often have lower solubility, conductivity, and voltage platforms [24, 30]. For the anode materials, most of the researchers tend to use Zn foil directly due to its higher corrosion resistance and capacity retention rate in comparison to Zn powder [31]. However, Zn dendrites may form on Zn foil anodes due to the imbalances in the electric field distribution [32, 33]. The presence of these dendrites intensifies the parasitic reaction of electrolyte decomposition, which contributes to the formation of more non-conductive by-products and results in increased electrode interface impedance [34]. It is also worth noting that continuous growth of dendrites eventually pierces the separator and cause short circuits inside the battery, leading to the rapid decay of battery capacity [35–37].

With regards to the separator materials, there is no specific commercial separator available for current ZIBs, and the glass-fiber nonwoven fabric remains the most commonly used separator in many recent studies [38]. However, the challenge is that the glass-fiber separator always suffers from structural damage during repeated cyclic processes due to its poor mechanical strength [39]. Thus, it is necessary to develop novel functional separators for high-quality ZIBs. For the electrolyte materials, aqueous-soluble Zn salts with a mildly acidic or neutral pH in solution are often chosen as the electrolyte in ZIBs. Among them, zinc sulfate ($ZnSO_4$) is one of the most conventional electrolytes by virtue of its low cost, high solubility, and excellent electrochemical properties. To meet the current demands of bendable or wearable devices, aqueous ZIBs are expected to possess both high energy density and exceptional mechanical flexibility. Therefore, the types and structures of electrode materials, combinations of the battery components, and physical conformation of ZIBs have been brought to our attention.

Materials in fiber-based structures have been gaining popularity for their potential uses because of their versatility in material combinations and structural designs, high mechanical flexibility, simple preparation methods, and numerous practical applications [40, 41]. Fibers are generally a kind of soft one-dimensional (1D) material with a large length-to-diameter ratio that can be manufactured into different dimensions or interwoven into a variety of structures for a wide range of applications [42]. With various breakthroughs in the development of fiber-based flexible energy harvesting, energy storage, sensing, and display devices, the potential of fiber-based and their assemblies in the energy field has been confirmed [43, 44]. Fiber-based materials can also be beneficial for every component of ZIBs as they allow softer, more efficient, and convenient applications [45–47]. In terms of the electrodes, nanofiber materials with exceptional flexibility and high specific surface area can provide a shortened diffusion pathway and sufficient active sites between the electrolytes and active materials of electrodes [48–50]. They can also adapt themselves to volume variations induced by the ion intercalation/deintercalation processes, achieving improved recycling stability [20, 51]. Besides, functional fibers like ceramics and polymers can ensure uniform and efficient ion conduction when acting as a separator material [52, 53]. More impressively, fiber-based materials with diverse morphologies can be employed to fabricate various constructions for flexible ZIBs [54, 55]. These fiber-based structures can greatly boost energy storage technologies especially for individualized flexible and wearable electronic applications.

In this review, we aim to provide a thorough overview of the concepts, principles, and applications of fiber-based materials for ZIBs. A variety of recently discovered fiber-based materials and their assemblies are highlighted in the fields of cathodes, anodes, current collectors, and separators, as illustrated in Fig. 1. Lastly, current challenges including electrochemical performances, large-scale production, and applicability of ZIBs in wearables are discussed, and the corresponding future research approaches are proposed. Moreover, the prospects of fiber-based ZIB manufacturing and their applications in flexible wearable electronics are reconnoitered. We believe that this review will serve as the fundamental guidance framework for the future development of fiber-based materials for ZIBs.

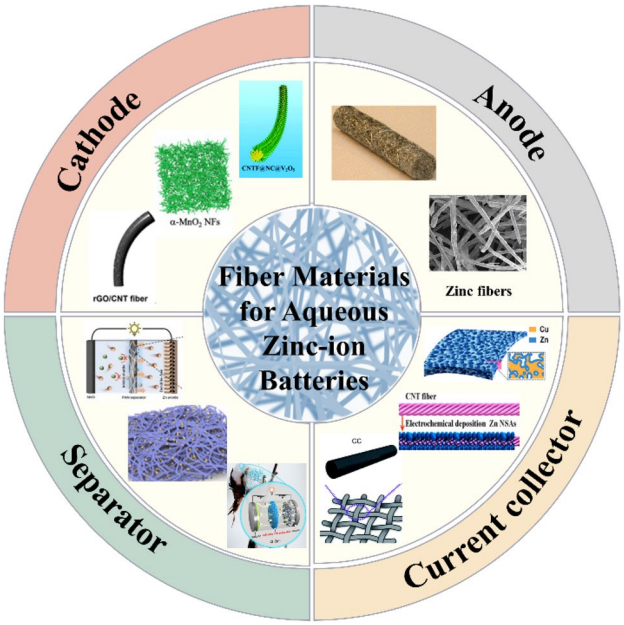

Fig. 1 Application of fiber-based materials in ZIBs

Fiber-Based Materials for Current Energy Storage Applications

Fiber-based structures have demonstrated great potential as one the most ideal candidates for developing functionally versatile materials for next-generation energy storage applications [56]. Fibers are known to have significantly a longer length than their width, and they can exist as nanofiber form having a diameter of less than one micrometer [57, 58]. The fiber morphology allows their conversion into multiple constructions including yarns, fibrous mats and fabrics for a number of purposes. It is also worth mentioning that fibers can be made from a diverse range of materials originated from natural or man-made sources. These features encourage their versatility in designing various battery components. For instance, recent studies have shown that many electrodes have been successfully developed by using metal-based, carbon-based, and polymer-based materials in fiber-based structures [59, 60]. One of the main advantages of fibers is their extremely high surface area to volume ratio, which increases the contact area between the electrolyte and the electrode, thus contributing to the increased utilization of surface active sites [61, 62]. In addition, the use of nanoengineered fiber-structured materials could promote mass transfer rates, resulting in smaller electrode polarization [63, 64]. Furthermore, the physical properties of these materials offer unparalleled benefits such as high mechanical flexibility and decent tensile strength, good stability and desirable durability in practical applications [65, 66]. Fiber-based materials manufacturing construction system is a long tradition in the textile sector, currently supported by sophisticated techniques. A number of functional homogeneous or composite fiber manufacturing and modification technologies are also available and accessible for different engineering applications [67]. Most of these are conducive to the manufacturing and development of high-performance ZIBs with fiber-based materials.

Fiber-Based Structures for Energy Storage Applications

Fiber can be a unit part for the construction of a wide range of 1D, 2D and 3D fiber assemblies, which offer high flexibility in fabricating different practical structures. Hence, functional and substrate materials in fiber-based structures have high potential of being manufactured into different dimensions or interwoven into a variety of constructions to provide a diversity of functions [68, 69]. It is also worth noting that the application of functional materials in constructing fiber-based structures endows the materials with better electrical, mechanical properties and physical attributes as opposed to the corresponding material in bulk forms [70, 71]. Numerous studies have already reported different fiber-based constructions of active materials for the production of advanced ZIB components [72]. For instance, functional materials can be converted into different constructions such as mono or composite fibers, yarns, fabrics, and fibrous mats [73, 74]. Therefore, more materials are able to be utilized in distinct parts of ZIBs based on their electrochemical and physical behaviors.

Commonly used functional types of fibers, such as core–shell or coaxial structured [75, 76], hierarchical structured [77], and helical fiber [78] have been applied for energy storage applications. Specifically, core–shell fibers with outer and inner compartments have the synergistic properties of the two types of materials used [79]. Hierarchically structured fibers with highly porous networks can facilitate fast electron/ion transport and high mass loading [80]. These fibers can also contribute to the good pliability and high flexibility of energy storage devices [75]. Moreover, fiber electrodes could be parallelly wound onto the substrate fiber to obtain a helical structured fiber with high tensile stability for ultra-stretchable energy storage application [81].

Yarn structures can yield better mechanical properties via twisting multiple yarns into helical or cable structures. For example, thin metal fibers may be twisted into more durable and flexible helical structured yarns, and the twisting process allows them to be employed in more demanding working environments. In addition, yarns made of distinct fiber materials can be constructed into a single yarn to gain synergistic features. A functional yarn can be twisted with another stretchable substrate yarn into a double-helix structured

material [81]. With higher tensile strength, uniformity, and abrasion resistance, the cable yarns enable themselves to be folded without breakage and significant loss of functions [82].

Fabrics, fibrous films, and fibrous porous networks can be formed by different construction techniques, mainly categorized into woven, knitted and non-woven types. For example, nanofibers can be woven into porous networks or fabrics to enhance active material loading and allow rapid electron transfer. Besides, nanofiber films can be produced by electrospinning, which is a cost and time-effective strategy to manufacture large-scale materials [83]. Moreover, the diverse fabric structure designs of functional materials contribute to the expansion of application fields. Notably, knitted structures can offer more remarkable stretchability than their woven or film counterparts. These fiber-based construction methods for functional materials can enhance the production feasibility and scalability of wearable electronics, pushing forward the development of flexible and durable energy storage devices.

Demand for Functional Fiber-Based Materials for ZIBs

Fiber-based functional materials have been gaining attention from various research groups attributing to their versatility and applicability for aqueous ZIBs [76]. Pristine metals, carbon, ceramics, polymers, and their composites have shown their necessity to be produced in fiber-based forms or incorporated into other fiber-based substrates for better electrochemical and mechanical performances, which can further encourage the development of efficient battery components for ZIBs.

Metal-Based Materials

Vanadium Vanadium oxide (V_xO_y) is known to be a popular cathode material used in ZIBs. They have garnered significant research attention owing to their high rate capacity, excellent rate capability, and outstanding cycle stability. Taking V_2O_5 as an example, it can achieve multiple redox reactions (*i.e.* V^{2+}, V^{3+}, V^{4+}, and V^{5+}) and provide a large ion transfer pathway with its specific layered structure and orthorhombic symmetry. One V atom coordinates with five O atoms to form a square pyramid chain with a shared corner. These pyramid chains are linked together to form layers, which can further be stacked on the *c*-axis to create a layered structure. The distance between these layers is 0.43 nm, which is sufficiently large for the intercalation of 0.074 nm Zn^{2+} ions. However, existing studies have consistently shown that low electrical conductivity and phase transformation of the V_2O_5 layered structure after Zn^{2+} intercalation may lead to capacity attenuation [84–86]. Furthermore, some studies have indicated that bulk V_2O_5 have a comparatively less stable structure, weaker ionic and electronic conductivity, and a lower ion diffusion coefficient for Zn^{2+} ions, resulting in unfavorable capacity loss [87]. Nevertheless, it is interesting to find that the limitations can be alleviated by the formation of nanostructures.

The nanostructure of active materials plays a key role in the activation process, capacity, and stability of electrode, and the adoption of nanostructures is one of the most effective ways to improve the electrochemical performance of V_xO_y cathode in aqueous ZIBs [88, 89]. The recent research on nanostructured V_xO_y cathode mainly includes nanobelts [90], nanopapers [91], nanowires [92–96], and nanofibers [97, 98]. It is worth noting that V_xO_y in nanofiber form possesses unique tunnel transport pathways with larger dimensions and causes fewer structural changes on Zn^{2+} intercalation, which is conducive to eliminating the limitations of solid-state diffusion of ions in the V_xO_y electrode [99]. In addition, these vanadium-based metal oxides may be grown onto fiber-based templates or loaded into other heterogenous substrate materials to form hybrid fiber-based structures with defect engineering for the enhancement of electrochemical performance [100]. The mesoporous composite nanofibers formed after calcination can greatly benefit Zn^{2+} insertion and permeability of electrolyte, which gives more satisfactory performance than its bulk counterparts [48]. V_xO_y in fiber forms has demonstrated remarkable performance, operational stability, and production feasibility in recent studies, and this deserves further investigation in fiber-based V_xO_y cathodes.

Manganese Manganese oxides (Mn_xO_y) are deemed as one of the most competent cathode materials in aqueous ZIBs. They may occur in variable valence states, which contribute to strong ion storage performance and high specific capacity. They can be produced in different crystallographic forms, including α-MnO_2, β-MnO_2, γ-MnO_2, and δ-MnO_2 [97, 101–105]. It is notable that α-MnO_2 has the higher theoretical capacity, voltage, and abundance among different forms. However, typical α-MnO_2 may suffer from severe capacity degradation if the battery is subjected to repeated charge–discharge cycles. In addition, the manganese-based materials including Mn_xO_y and their composites are also low-priced, low-toxic, and sustainable resources. Nevertheless, the poor intrinsic electronic conductivity, proton transport and electrolyte penetration of Mn_xO_y reduce its specific capacitance [106]. Therefore, the issues concerning rapid capacity fading and sluggish transport kinetics should be addressed before adopting this material for practical applications.

Approaches like physical doping and nanoengineering are commonly employed to improve the properties of Mn_xO_y. In situ fabrication of Mn_xO_y composites with carbons and

polymers can be utilized to improve the rate and cycle performances of the manganese-based cathode in ZIBs [107, 108]. More so, the nanostructures of Mn_xO_y like nanofibers and nanowires on fiber-based hosts can shorten the ion and electron transport pathways, and these constructions can maintain higher mechanical integrity for a wider range of practical applications when compared with the bulk forms. Fiber-based structures of Mn_xO_y manifest their improvement in electrochemical reversibility and stability, thus the rate capability and capacity retention of batteries can be enhanced. For example, α-MnO_2 in nanofiber form can be synthesized using the hydrothermal method and applied as a cathode in Zn/MnO_2 battery and exhibits excellent rate capability and high-capacity retention of 92% after 5,000 cycles [97]. Although the electrodeposition and hydrothermal methods offer outstanding results, scaling up the actual manufacturing process is still challenging. Furthermore, the tap density of nanosized MnO_2 generated by electrodeposition and hydrothermal techniques is relatively lower, leading to a considerable reduction in cell-level energy density. Fiber forms of cathode materials have shown more prominent electrochemical performance, yet more effort is still required to address the existing limitations.

Other Metals and Metal Oxides Nanostructured molybdenum trioxide (MoO_3) is another extensively studied transition-metal oxide, and it is also a recently highlighted material in electrochemical storage. Orthorhombic α-MoO_3 is in a thermodynamically stable phase with a layered structure parallel to (010), which allows guest atomic ions to insert splitters between the layers [109]. Thus, MoO_3 holds great promise for the high-performance cathode electrode in ZIBs. Nevertheless, the electrochemical instability of orthorhombic MoO_3 nanowires can be induced by severe destruction and dissolution of active substances in an aqueous electrolyte [110]. To alleviate this impact, surface engineering of MoO_3 like coating and phosphating process, or electrolyte engineering may be employed to allow more decent capacity retention, better cyclic stability, more rapid charge transport, and higher surface reactivity. Fiber-based substrates may offer property enhancement to the molybdenum-based oxides. To be more specific, carbon cloth can increase the surface area and electron mobility of the coated α-MoO_3 to overcome the intrinsic limitations including retarded faradaic kinetics and mass transport [111]. Porous mats fabricated with nanobelts or nanofibers provided a considerable amount of interface for the reaction between active materials and electrolyte [112].

Metal materials generally possess excellent conductivity and mechanical strength; therefore they are potential candidates for the preparation of the battery components, especially current collector and supporting framework for yarn-shaped battery. The fiber-based structures like the yarn form of stainless steel offer superior strength, conductivity, corrosion resistance, thermal stability, and higher flexibility compared to conventional cellulose yarns [113]. Thus, they can act as a reliable electrode substrate for the deposition of anode and cathode materials [114]. For instance, highly porous iron fibers have great mechanical integrity and connectivity within their fibrous structure, and this iron fibrous material can provide high conductivity at a lower cost [115]. Furthermore, the remarkable conductivity and tensile properties of silver fibers enable them to be adopted as another efficient current collector [81]. To increase the flexibility of the yarn-shaped electrode, metal material can deposit on another soft material to obtain a conductive and flexible electrode [116]. Fiber-based structures can widen the structural designs of metal-based materials, which further provide more compatible components for a high-performance battery.

Carbon and Ceramic-Based Materials

Carbon materials are mostly strong, stable, and compatible with various materials, which are favorable for the formation of composites [117, 118]. They are available in various types of physical and chemical structures, and thus are universally found in the ZIB components for enhanced electrochemical functionality, structural flexibility, and mechanical integrity. Carbon materials usually serve as functional dopants, substrates, frameworks, or active surface ingredients to promote the electrochemical performance of the battery. The fiber-based structures of these versatile materials offer a multitude of advantages, mainly including functional enhancement and wider practical designs. One of the distinguished improvements of ZIB components with carbon materials is the minimization of dendrite growth of Zn. Recent studies have indicated that hierarchical nanofiber-based current collector substrate materials gained a higher electroactive surface area and more uniform electric field, resulting in the efficient inhibition of Zn dendrite growth [30]. In addition to Zn anodes, carbon fiber materials can assist the promotion of stability and redox kinetics in cathodes.

In particular, carbon nanotube (CNT) and carbon cloth fiber-based structures are widely found in recent energy storage studies, owing to their outstanding electrochemical performance and mechanical advantages. CNT fibers constructed with aligned CNTs can inherit the advantages of CNTs and show an additional property of macroscopical mechanical flexibility, exhibiting greater potential for wearable electronics. CNT fibers together with templates like metal–organic framework (MOF) can also form a highly conductive 3D nitrogen-doped porous carbonaceous skeleton. This core–shell hierarchical structure enables mass loading of active materials onto the fiber-shaped cathode without the use of binders, favoring the improvement in

volumetric capacity, electronic conductivity, and diffusion efficiency of the ZIB system [119]. Moreover, a CNT-based framework for pristine α-MnO_2 can increase the tapped density of α-MnO_2, which enhances the cell-level energy density [20]. Furthermore, carbon cloth, a 2D fabric made of carbon fiber, offers a softer alternative to stainless-steel foil. It offers outstanding mechanical strength, lightweight structure, and excellent electrical conductivity for more demanding applications.

To enhance the performance of carbon materials, different modification techniques or assemblies of multiple materials can be adopted. Flexible carbon nanofibers may be modified easily via embedding functional ingredients within the carbonaceous matrix [83] or surface engineering, with deposition technologies. Different combinations of carbon-based fibers and nanosheets can be potentially used as ZIB components for wearable applications. For example, single-walled CNT fibers and reduced graphene oxide (rGO) nanosheets are good complementary materials. Mesoporous CNT fibers can prevent restacking between rGO nanosheets, thus increasing the surface area. On the other side, rGO nanosheets can endow CNT fibers with better electrical conductivity [120]. With all these beneficial properties, ease of modification and integrability, fiber-based carbon materials are ideal for preparing various cathodes, anodes, and current collectors to improve the energy storage performance and practicability of ZIBs.

Ceramic materials usually have good hardness, low thermal expansion, and great chemical resistance. Their extensive range of physical and chemical properties means that they are suitable for use as ZIB components. Glass fiber (GF) is one of the mostly used separators for ZIBs. The fibrous fabric endows GF with a higher surface area for better absorption of electrolytes, contributing to better ionic transportation. Nonetheless, GF separator has low mechanical strength and uneven large pores, thereby the formed Zn dendrites have a high chance to pierce through the fragile GF separator, eventually causing a short circuit in the cell [121]. Therefore, modification strategies like decorating GF materials with polar constituents, vertical graphene, GO and nitrogen-doped carbon should be adopted to enhance the mechanical properties and optimize their performance. Besides, Na super-ionic conducting (NASICON)-type, and Li super-ionic conducting (LISICON)-type ceramics are normally used as crystalline solid electrolytes, and some studies have started to explore their potential as separators in liquid electrolyte batteries [122].

Polymer-Based Materials

The majority of the natural and synthetic polymeric materials can be easily manufactured into a variety of fiber-based constructions using well-established technologies. Most of these polymers are commercially available at reasonable prices and are thus favorable for large-scale production. More importantly, a considerable number of studies have shown their advantageous modifiability in versatile applications.

Naturally occurring organic polymers like cellulose and protein are abundant and renewable, so they encourage the sustainable production of functional fiber-based materials. Cellulose fibers, the most prevalent natural organic polymer on the planet, have high mechanical strength, good hydrophilicity, decent insulation performance, and favorable biodegradability [123]. Their homogeneous porous morphology and rich hydroxyl groups also contribute to their use as separators [124]. In addition, numerous studies of advanced natural fiber materials could be served as references for fiber modification. For example, their properties may further be enhanced with the incorporation of ceramic materials like high dielectric constant zirconium dioxide (ZrO_2) that can aid Zn plating/stripping [53]. Furthermore, cellulose can be a pore builder for channelling electrolytes and an internal wicking agent for extending the operation period of the Zn anode [125].

Most synthetic polymers have the advantages of mechanical flexibility to withstand applied force, versatility to customize functional groups, and good modifiability to be produced by novel processing technologies [126]. For instance, polyacrylonitrile (PAN) and polyacrylamide (PAM) can be utilized for the production of solid-state electrolytes in ZIBs. Most of the polymers can easily be chemically modified and physically shaped into the desired 3D hierarchical structures for better ionic conductivity, flexibility, and mechanical strength [127]. Furthermore, conductive polymers with a conjugated character like polypyrrole (PPy) and poly(3,4-ethylene dioxythiophene) (PEDOT) can confer other materials with better electrical conductivity, capacity and redox reversibility for developing flexible electronics [170]. In addition to the interactions between anions and oxidized nitrogen-containing groups in PPy, cations can also be stored in reduced nitrogen-containing groups for providing additional capacity. Hence, the conductivity of the cathode can be greatly improved by using a conductive polymer fiber cathode in ZIBs. The versatility and tunability of fiber-based structures holds a promising prospect in structural designs of high-performance ZIBs.

Organic Materials

Furthermore, organic material is another kind of attractive cathode candidate for ZIBs due to their structural versatility, sustainability and light weight [128]. However, the organic cathode materials suffer from low conductivity, severe structural damage and dissolution problems in the electrochemical process, which result in unsatisfactory rate

performance and unreliable cycle durability. These limitations can be alleviated by the adoption of nanostructures and quinone-containing materials. Nanofibrous membrane endows the organic cathode materials with a greater number of micro and nanopores, contributing to a higher interfacial contact area between the electroactive groups and electrolytes [129]. It is worth noting that organic cathodes with quinone compounds exhibit higher capacity with a lower solubility in aqueous conditions [25]. Moreover, developing organic–inorganic hybrid cathode material with a dual energy-storage mechanism is another strategy to enhance the cycling stability of organic materials.

Preparation Method of Fiber-Based Materials

The preparation of functional fiber-based materials involves different types of physical and chemical fabrication approaches. Fiber-based forms of synthetic and organic materials can be manufactured and functionalized with sophisticated techniques such as spinning, hydrothermal synthesis, deposition, and template-assisted fabrication of homogeneous or heterogeneous materials. The modification or functionalization of the raw materials may be achieved at the pre-, mid-, or post-stages of fiber formation depending on the material types and functions required. Since spinning and chemical synthetic techniques have been extensively studied, they enable the controlled synthesis of fiber-based materials with specific diameters, morphologies, tensile properties, and chemical functions. In addition, multiple techniques may be utilized to fabricate more complicated morphologies and compositions. Different homogeneous metals, metal oxides, carbon, ceramics, polymers or their composites can be employed to produce functional materials in fiber forms using the aforementioned strategies, allowing these materials to be used in a wider range of work environments.

Spinning Approach

Spinning is a simple and effective method for the large-scale production of fibers. In recent years, electrospinning has been commonly adopted to produce functional nanofibers using polymeric materials doped with active ingredients, or sol–gel-derived materials for ZIB components. Electrospun materials can be prepared with a spinneret and injection syringe for extruding the polymeric solution at a constant rate, a high-voltage power supply for charging the polymeric droplets, and a charged metal collector for receiving the nanofibers drawn by different forces including electrostatic force, viscoelastic force and air drag force [130], as illustrated in Fig. 2a. The fiber diameter, material dimension and density can be simply tuned with the parameters of the electrospinning setup. This technology can efficiently prepare 1D nanofibers, 2D nonwoven films, and 3D frameworks with fiber diameters at the micro and nano levels [131]. It is also easier to obtain fibrous films with higher porosity via random stacking of electrospun nanofibers. The porous structures are beneficial for ion migration throughout the network, which improves the conductivity performance of the battery. In addition, carbon-based fibrous networks with rich mesoporous structures can also be prepared by the calcination of electrospun polymeric fibers. These electrospun fibers have a large surface area-to-volume ratio and good flexibility to accommodate various configurations [132]. Besides, carbon nanofiber arrays are conventionally drawn through dry spinning. Fine metal fibers can also be prepared by spinning at excessively high temperatures, and they can subsequently be transformed into yarn structures with the use of twist-bundle drawing. Furthermore, some composite structures

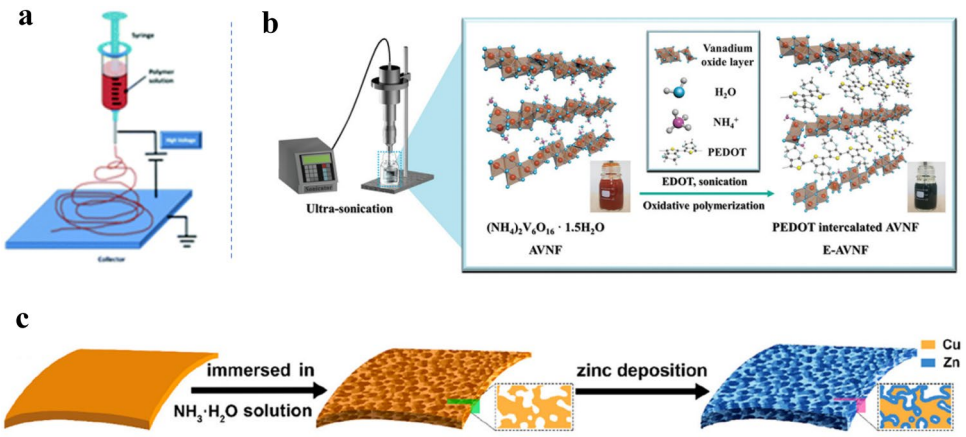

Fig. 2 Schematic illustration of **a** fabricating nanofibers with electrospinning setup; Reproduced with permission from ref [133], Copyright 2015, The Royal Society of Chemistry. **b** intercalation of PEDOT and ammonium ions into vanadate layers via sonication; Reproduced with permission from ref [134], Copyright 2021, Wiley–VCH. and **c** preparing 3D porous Zn anode by using an etched copper template; Reproduced with permission from ref [135], Copyright 2019, American Chemical Society

like core–shell fiber may be attained by coaxial electrospinning or wrapping a tough supporting fiber with functional electrospun nanosheets.

Synthetic Chemical Approach

The chemical approaches of fabricating nanofibers to improve the resultant functionality of materials have been successfully demonstrated in numerous studies. The hydrothermal method is one such promising strategy to prepare nanofibers in a considerable number of scenarios. The hydrothermal method generally involves the dissolution and recrystallization of heterogeneous substances in solvent within an enclosed reactor under high temperature and high pressure, which can facilitate the growth of primary particles to nanofibers [136]. The virtues of this method include high quality fabricated nanofibers, mild synthetic conditions, and good homogeneity [132]. Formation of nanofibers may be subsequently followed by the facile vacuum filtration method to form a nanofibrous film. In addition, the sonochemical method can assist with the intercalation of foreign materials like conducting polymers and ions into the nanofiber crystal lattice of transitional metal oxide cathode for improving electrical conductivity, as shown in Fig. 2b [134].

Deposition, in particular chemical vapor deposition (CVD) and electrodeposition, allows both uniform formations of functional materials on fiber-based substrates and controls the growth of active materials in the nanofibrous form using chemical vapor or electric current [137]. Deposition methods can be applied to versatile types of active and substrate materials, and these methods also promote the formation of binder-free electrodes. Besides, low-cost coating-based methods like dip-coating can be adopted for soluble or solution-processible materials [138]. For the preparation process, templates are commonly used to assist the fabrication of functional fiber-based materials as they can efficiently guide the growing direction of active materials into predefined morphology. Specific structures such as 3D hierarchical skeleton and porous structures can be developed through the use of templates like MOFs, carbon nanofibers, nickel foams, and 3D porous copper materials [133, 135, 139]. They offer a simple way to produce structures with a large surface area for both electrical conductivity and mass loading of active ingredients. For instance, a 3D porous copper skeleton was prepared by chemical etching method for Zn deposition, as shown in Fig. 2c.

Applications of Fiber-Based Materials for ZIBs

Fiber-based structures have demonstrated great potential and many application possibilities in advanced functional materials. In this study, we focused on the multitude of applications of fiber-based materials in ZIB components, namely cathodes, anodes, current collectors, separators, and electrolytes.

Fiber-Based Materials as Cathodes

Vanadium-Based Fiber Cathodes

Nanostructured V_2O_5 cathodes used in the assembly of aqueous ZIBs have become one of the most effective ways to improve electrochemical performance [89]. The electrochemical performances of vanadium-based cathodes with different nanostructures are summarized in Table 2, and the nanofibers have been identified to have better electrochemical activity among these nanostructures. Following the compact nature of V_2O_5 cathodes, Yang et al. studied the intercalation pseudo-capacitance behavior and ultrafast kinetics of Zn^{2+} in the unique tunnels of VO_2 nanofibers in aqueous ZIBs, as shown in Fig. 3a [99]. The VO_2 nanofibers endowed a high and stable reversible capacity of 357 $mAh{\cdot}g^{-1}$, which was much higher than that of its raw material of bulk V_2O_5 (<300 $mAh{\cdot}g^{-1}$) [140]. Moreover, VO_2 nanofibers maintained satisfactory capacity even at a high current density of 300 C.

Electrospinning is one of the most widely used methods for the large-scale production of V_xO_y nanofibrous cathode materials. Volkov et al. proposed a sol–gel electrospinning method for the preparation of V_2O_5 nanofibers with an average diameter of 390 nm (Fig. 3b) [49]. The resultant cathode material was used for rechargeable ZIBs, and a high specific capacity of up to 282 $mAh{\cdot}g^{-1}$ was obtained with remarkable electrochemical stability after 500 cycles. The excellent electrochemical performance of the sol–gel electrospun cathode was attributed to the robust surface chemistry combined with the intercalation pathway, resulting in the overall increase of the specific capacity. In addition, the contribution of Zn ion intercalation could be magnified by the water molecule insertion into the material structure, which could shorten the initial activation process.

Based on the shortened initial activation process, Chen et al. further constructed porous V_2O_5 nanofibers via calcination of the electrospun fibers [48]. The calcined fiber-like material exhibited a richly mesoporous structure, which greatly favored the electrolyte permeation and Zn^{2+} insertion, as illustrated in Fig. 3c. This V_2O_5 nanofibers in such open and stable structure produced a highly reversible capacity of 319 $mAh{\cdot}g^{-1}$ at 20 $mA{\cdot}g^{-1}$ with a capacity retention of 81% over 500 cycles. More so, V_2O_5 nanofibers with 3D porous structures could be rationally synthesized by electrospinning with PAN and the subsequent pyrolysis. Functional physical defects like pore pathways and caves could be developed within the carbonized fiber skeletons, and chemical defects on V_xO_y were created synchronously

Table 2 Comparisons of the electrochemical performances of the typical reported vanadium-based cathodes formed with different materials in various nanostructures

Cathode material	Electrolyte	Specific capacity	Energy/power density	Cycling performance	Ref
VO_2(B) nanofibers	3 M $Zn(CF_3SO_3)_2$	357 mAh·g^{-1} at 0.1 A·g^{-1}	297 Wh·kg^{-1} at 180 W·kg^{-1}	91.2% retained after 300 cycles at 5 C	[99]
V_2O_5 nanofibers	3.5 M $ZnSO_4$	357 mAh·g^{-1} at 0.05 A·g^{-1}	–	36% retained after 500 cycles	[49]
Porous V_2O_5 nanofibers	3 M $Zn(CF_3SO_3)_2$	319 mAh·g^{-1} at 20 mA·g^{-1}	–	81% retained after 500 cycles at 588 mA·g^{-1}	[48]
CNTF@NC@ V_2O_5	gel electrolyte	457.5 mAh·cm^{-3} at 0.3 A·cm^{-3}	40.8 mWh·cm^{-3}/ 5.6 W·cm^{-3}	85.3% after 400 cycles	[119]
$Na_3V_2(PO_4)_3$ nanoparticles	0.5 M $Zn(CH_3COO)_2$	97 mAh·g^{-1} at 50 mA·g^{-1}		74% retained after 100 cycles at 50 mA·g^{-1}	[141]
$Na_{1.1}V_3O_{7.9}$ nanoribbons	1 M $Zn(CF_3SO_3)_2$	223 mAh·g^{-1} at 300 mA·g^{-1}	–	92.6% retained after 500 cycles at 1 A·g^{-1}	[142]
V_2O_5·nH_2O	3 M $Zn(CF_3SO_3)_2$	372 mAh·g^{-1} at 300 mA·g^{-1}	90 Wh·kg^{-1}/ 6.4 kW·kg^{-1}	71% retained after 900 cycles at 6A·g^{-1}	[16]
$Zn_3V_2O_7(OH)_2$·2H_2O	1 M $ZnSO_4$	213 mAh g^{-1} at 50 mA·g^{-1}	214Wh·kg^{-1}	68% retained after 300 cycles at 200 mA·g^{-1}	[143]
CuV_2O_6 nanobelt	$ZnSO_4$	427 mAh g^{-1} at 0.1 A·g^{-1}	317 Wh·kg^{-1}	99.3% after 3,000 cycles at 5 A·g^{-1}	[90]
V_2O_5 nanopaper	2 M $ZnSO_4$	341.3 mAh·g^{-1} at 1.0 A·g^{-1}	277.5 Wh·kg^{-1}	76.9% retained after 500 cycles at 10 A·g^{-1}	[91]
V_2O_5 nanowires	3 M $ZnSO_4$	276 mAh·g^{-1} at 1.0 A·g^{-1}	–	55% retained after 500 cycles at 1 A·g^{-1}	[92]
$H_2V_3O_8$ Nanowire/Graphene	3 M $Zn(CF_3SO_3)_2$	394 mAh·g^{-1} at 1/3 C	168 Wh kg^{-1} at 1/3 C	87% after 2,000 cycles	[93]
$V_6O_{13-\delta}$ nanowires	polymer electrolyte		max. 231 mWh·cm^{-3}	97% after 1,000 cycles at alternative 13 and 4 A·g^{-1}	[94]
CuV_2O_6 nanowire	3 M $Zn(CH_3F_3SO_3)_2$	338 mAh·g^{-1} at 100 mA·g^{-1}	74 Wh·kg^{-1}	100% retained after 1,200 cycles at 5 A g^{-1}	[95]
ZnVO nanowire	3 M $Zn(CF_3SO_3)_2$	140 mAh·g^{-1} at 2 A·g^{-1}	–	77.1% retained after 700 cycles at 2A g^{-1}	[96]
E-AVNF nanofiber	2.5 M $Zn(CF_3SO_3)_2$	344 mAh·g^{-1} at 0.5 A·g^{-1}	124 Wh·kg^{-1} at 16,000 W·kg^{-1}	94% retained after 1,000 cycles at 10 A·g^{-1}	[134]
V_2O_5 nanofibers	3.0 M $Zn(OTf)_2$	211.36 mAh·g^{-1} at 100 mA·g^{-1}	–	–	[98]

via the pyrolysis process of individual PAN fiber. When used as a cathode, the V_2O_5 nanofibers enabled capacity retention of 83% after 1,000 cycles at 5 A·g^{-1} [100]. Furthermore, two transition metal oxides including $Zn_2V_2O_7$ and V_2O_5 in poly(methyl methacrylate) were used to make the core covered with PAN shell, which gave a 1D hybrid fiber, with a central hollow shell and an inner carbon network after carbonization [75]. The core–shell hierarchical structure allowed quick electron/ion transit and high mass loading of the oxides, while the 1D structure ensured pliability and flexibility. It was shown that hybrid fibers containing the active materials had better electrochemical characteristics and higher rate capabilities.

Constructing a 3D skeleton by template method has proved to be another effective strategy to increase the electrochemical properties of electrode materials [144]. Due to their immense surface area, high porosity, and rich carbon content, MOFs have been proven to be viable templates for generating 3D carbon skeletons with excellent conductivity [139]. For instance, a fine core–shell nanocomposite could be created with 3D porous nitrogen-doped carbon nanoarrays derived from ZIF-67 on a CNT substrate fiber as the core and 2D thin V_2O_5 nanosheets as the shell. The unique hierarchical core–shell structure not only increased the mass loading of V_2O_5 nanosheets (Fig. 3d), but also improved electron transport and ion diffusion, thus gaining greater volumetric and specific capacity, and higher rate capability [119].

Another simple method for preparing nanofibrous cathode materials is hydrothermal synthesis. Kheawhom et al.

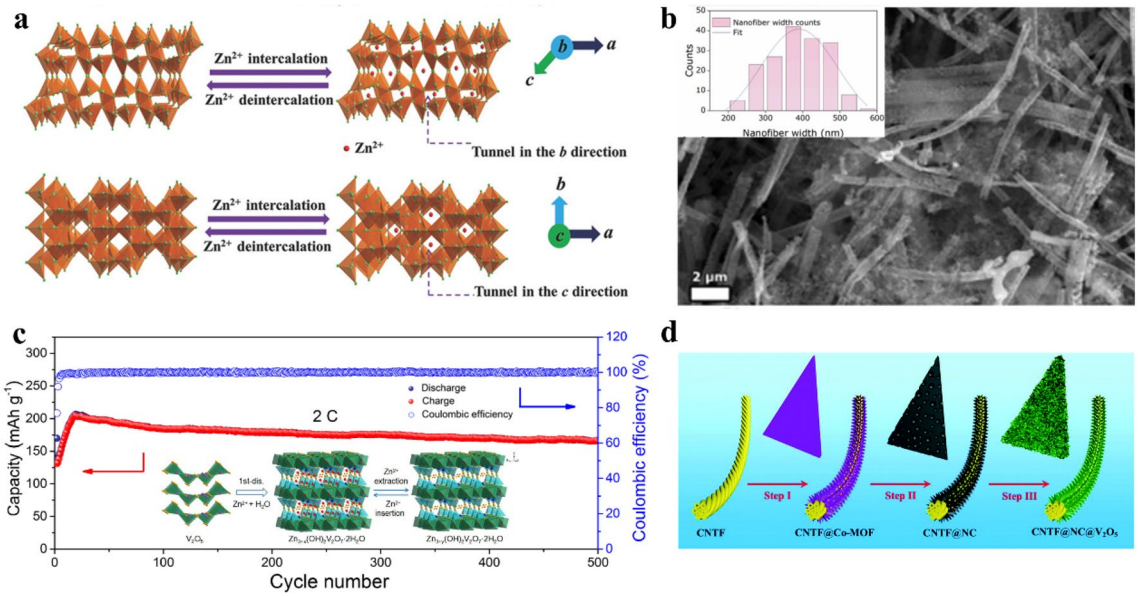

Fig. 3 **a** Schematic view of Zn^{2+} intercalation/de-intercalation with VO_2 (B) nanofibers projected along the direction of the *b*- and *c*-axes; Reproduced with permission from ref [99], Copyright 2018, Wiley–VCH. **b** scanning electron microscope (SEM) image of annealed V_2O_5-nanofibers and distribution chart of nanofibers diameter; Reproduced with permission from ref [49], Copyright 2021, Elsevier. **c** Long-term cycling performance of porous V_2O_5 nanofibers cathode at a current density of 2 C; Reproduced with permission from ref [48], Copyright 2019, Elsevier. and **d** Schematic illustration of the formation mechanism of the NC@V_2O_5 hierarchical core–shell structure on a CNT fiber; Reproduced with permission from ref [119], Copyright 2013, The Royal Society of Chemistry

explored unique binder-free, centimeter-long, and single-crystal V_2O_5 nanofibers (BCS-VONF) for the fabrication of ZIB cathodes [98]. BCS-VONF on carbon fabric could be produced using a simple one-step hydrothermal process. The usage of a binder-free electrode could reduce the electrode weight, avoid the use of hazardous solvents, and improve electrochemical performance. To address the issue of random and uncontrolled interlayer distance with vanadium-based materials, Ahn et al. presented a simple sonochemical approach for regulating the interlayer of the vanadate nanofiber crystal structure with PEDOT [134]. The conducting polymer intercalation helped to increase the number of active sites on the vanadate, and speed up the Zn^{2+} ion intercalation/de-intercalation process by extending the electron channel and widening the distance between the vanadate layers.

Manganese-Based Fiber Cathodes

α-MnO_2 delivers superior electrochemical performance due to its large size of spinel [2 × 2] and [1 × 1] [51]. As shown in Fig. 4a, the [2 × 2] tunnel structures along the *c*-axis consist of four MnO_6 octahedral elements with shared edges. The large spinel sizes allow ions to be inserted, which can determine the electrochemical performance of MnO_2. In addition, in-situ methodologies have been used to develop composite materials containing carbon and manganese-based oxides for ZIBs to increase the rate and cycle performances, which can improve the practicability of manganese-based cathodes [145]. For example, MnO_2 nanowires anchored with graphene quantum dots (GQDs) have been devised and explored as a cathode material for ZIBs to address issues like rapid capacity fading and slow transport kinetics [146]. As shown in Fig. 4b, the increased amount of GQD component can greatly enhance the cycling stability of MnO_2 cathode by accelerating the transport kinetics and inhibiting the manganese dissolution.

Notably, Ren et al. attempted to coat α-MnO_2/rGO nanowires with conductive polypyrrole (PPy) via in situ self-polymerization [51]. It demonstrated that the PPy coating layer not only stabilized the structure of α-MnO_2 but also enhanced the conductivity of the composite cathode. In addition, rGO grown on α-MnO_2 provided additional adsorption sites for Zn^{2+}, which could further improve the capacity of cathode materials. Specifically, α-MnO_2/rGO-PPy maintained a reversible capacity of 213.8 mAh·g^{-1} for 100 cycles at 0.5 A·g^{-1}, more superior to those of α-MnO_2/rGO and α-MnO_2. Furthermore, Liu et al. proposed a simple and scalable chemical precipitation/spray granulation process (Fig. 4c) for the production of α-MnO_2 nanofibers/CNT integrated microspheres as a cathode material for aqueous ZIBs [20]. When compared to pristine α-MnO_2, α-MnO_2 uniformly anchored on the CNT framework could display

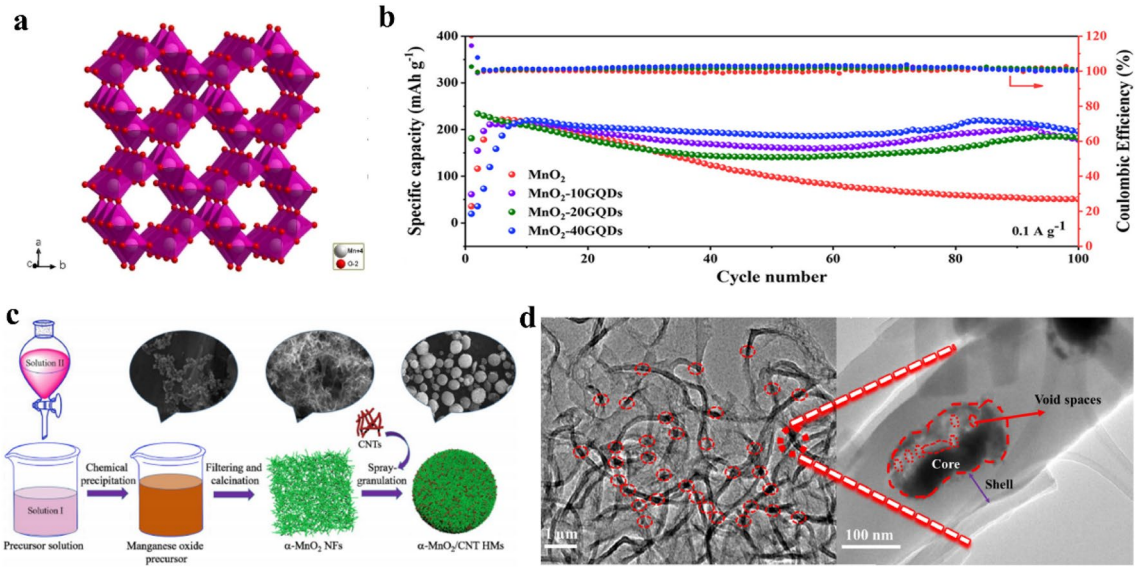

Fig. 4 **a** The crystal structure of α-MnO_2 with MnO_6 octahedral units, in which the small spheres (red) represent O and the large spheres (gray) represent Mn; Reproduced with permission from ref [51], Copyright 2021, Springer Nature. **b** Cycling performance with the Coulombic efficiency of MnO_2, MnO_2-10GQDs, MnO_2-20GQDs, and MnO_2-40GQDs; Reproduced with permission from ref [146], Copyright 2021, American Chemical Society. **c** Schematic illustration of the preparation of α-MnO_2 nanofibers (NFs) and α-MnO_2/CNT hierarchically assembled microspheres (HMs) and SEM images of the corresponding products at different synthetic stages; Reproduced with permission from ref [20], Copyright 2019, Elsevier. **d** Transmission electron microscope (TEM) image of the Mn_3O_4@HCFs-7.5 and the magnified TEM image of a concerned area of Mn_3O_4@HCFs-7.5; Reproduced with permission from ref [147], Copyright 2020, Elsevier

considerably higher tap density, thus effectively improving the electrochemical stability.

Lately, electrospinning technology is widely adopted to produce hierarchically porous nanofibrous films for manganese-based applications. For instance, Yang et al. [147] synthesized a core–shell structure cathode by encapsulating Mn_3O_4 nanoparticles in the carbon fibers (Mn_3O_4@C) via coaxial electrospinning and carbonization, as shown in Fig. 4d. Different samples were generated and examined in this study by altering the concentration of precursor PAN. The highly porous amorphous carbon shell and a large number of core void spaces of Mn_3O_4@C contributed to the long-term cyclability. A specific amount of carbon shell not only served as a barrier layer to prevent Mn_3O_4 from dissolving into the electrolyte but also altered the surface of the active elements to assist the uniform current flow in the electrode. Similarly, Wu et al. developed MnO@N–C composite fibers using manganese(II) acetate and poly(vinyl pyrrolidone) through electrospinning, followed by annealing [150]. The MnO@N–C cathode possessed a reversible capacity of 176.3 $mAh{\cdot}g^{-1}$ at 500 $mA{\cdot}g^{-1}$, even after 200 cycles, and 100.5 $mAh{\cdot}g^{-1}$ in a large current density of 1.2 $A{\cdot}g^{-1}$. For revealing the current progress, the electrochemical behaviors of manganese-based cathodes with different fiber-based structures and composite materials were summarized in Table 3. It is obvious that the crystal types and morphologies had a significant impact on the capacity and cycling characteristics of Mn_xO_y. More efforts are expected to further optimize the related structures to achieve long-term cycling stability for practical application.

Other Material Cathodes

Structural carbon materials like carbon nanofibers have been widely adopted in electrochemical energy conversion and storage devices owing to their superior mechanical, electrical, and chemical capabilities. Using two types of rationally designed fiber electrodes, Chen et al. have recently achieved the first quasi-solid-state Zn-ion hybrid fiber capacitors (ZnFC) [120]. The cathodes were CNT/GO composite fibers formed hydrothermally in capillary columns, whereas the anodes were graphite fibers coated with a thin layer of Zn metal. The assembled ZnFC demonstrated ultrahigh volumetric energy density, long cycling life, and outstanding mechanical flexibility under different deformation conditions. Notably, the ZnFC showed superior cycling stability of 98% capacitance retention after 10,000 cycles, and it could be easily integrated into flexible devices to provide a promising energy storage solution for wearable electronics. Similarly, Jian et al. constructed flexible core–shell diamond/carbon fibers for a binder-free positive electrode [156]. Diamond/Zn supercapacitor, using flexible diamond fibers as cathode and current collector, also possessed excellent gravimetric and volumetric energy densities, and also

Table 3 Comparisons of the electrochemical performance of the typical reported manganese-based cathode materials for aqueous ZIBs

Cathode material	Electrolyte	Specific capacity	Energy/power density	Cycling performance	Ref
α-MnO_2 nanofibers /CNT	0.1 M $MnSO_4$	296 mAh·g^{-1} at 0.2 A·g^{-1}	0.98 Wh·cm^{-2} at 0.2 A·g^{-1}	96% retention over 10,000 cycles at 3 A·g^{-1}	[20]
α-MnO_2 nanofiber	2 M $ZnSO_4$ + 0.1 M $MnSO_4$	285 mAh·g^{-1} at 1.44 V	170 Wh·kg^{-1} at C/3	92% over 5,000 cycles at 1.44 V	[97]
MnO_2@CNT composite fiber	PAM	302.1 mAh·g^{-1} at 60 mA·g^{-1}	53.8 mWh·cm^{-3}	98.5% retained after 500 cycles at 2 A·g^{-1}	[36]
MnO_2-40GQD	2 M $ZnSO_4$ + 0.2 M $MnSO_4$	295.7 mAh·g^{-1} at 0.1 A·g^{-1}	–	88.99% after 100 cycles at 0.1 A·g^{-1}	[146]
α-MnO_2/rGO nanowires	3 M $Zn(CF_3SO_3)_2$	248.8 mAh·g^{-1} at 0.5 A·g^{-1}	–	85.9% after 100 cycles at 0.5 A·g^{-1}	[51]
α-MnO_2	1 M $ZnSO_4$ or 1 M $Zn(NO_3)_2$	210 mAh·g^{-1} at 105 mA·g^{-1}	–	77% retained after 100 cycles at 1,260 mA·g^{-1}	[148]
MnO_2 nanospheres	2 M $ZnSO_4$ + 0.1 M $MnSO_4$	275 mA·g^{-1} at 0.3 A·g^{-1}	161 Wh·kg^{-1}at 5.7 kW·kg^{-1}	56 mAh·g^{-1} after 600 cycles at 0.3 A·g^{-1}	[22]
$ZnMn_2O_4$	3 M $Zn(CF_3SO_3)_2$	150 mAh·g^{-1} at 500 mA·g^{-1}	70 Wh·kg^{-1}	94% retained after 500 cycles at 500 mA·g^{-1}	[149]
β-MnO_2	$Zn(CF_3SO_3)_2$	225 mAh·g^{-1}	75.2 Wh·kg^{-1}	94% retained after 2,000 cycles	[101]
Mn_3O_4@HCFs	2 M $ZnSO_4$ + 0.15 M $MnSO_4$	215.8 mAh·g^{-1} at 0.3 A·g^{-1}	225.8 Wh·kg^{-1}	96.9% retained at 400 mA·g^{-1} after 1300 cycles	[147]
MnO@N–C	2 M $ZnSO_4$	249.5 mAh·g^{-1} at 0.1 A·g^{-1}	–	70.7% retained after 200 cycles at 200 mA·g^{-1}	[150]
PANI-MnO_2	2 M $ZnSO_4$ + 0.1 M $MnSO_4$	280 mAh·g^{-1} at 200 mA·g^{-1}	–	90% retained after 200 cycles at 200 mA·g^{-1}	[151]
δ-MnO_2 nanoflake	1 M $ZnSO_4$	250 mAh·g^{-1} at 83 mA·g^{-1}	–	100% during 100 cycles	[104]
γ-MnO_2/rGO	2 M $ZnSO_4$ + 0.2 M $MnSO_4$	230 mAh·g^{-1} at 0.4C	–	80% retained after 200 cycles at 0.4C	[105]
MnO_2@CNT fiber	Zn salt	322 mAh·g^{-1} at 0.1 A g^{-1}	437 Wh·kg^{-1}	85% retained after 100 cycles	[82]
MnO_2@CNT paper	2 M $ZnSO_4$	121 mAh·g^{-1} at 0.1 A·g^{-1}	84 Wh·kg^{-1} at 0.2–1.8 V	91% retained after 1,000 cycles at 1 A·g^{-1}	[152]
PPy-MnO_2@SS yarn	gel	143.2 mAh·g^{-1} at 1 C	–	60% retained after 1,000 cycles at 2 C	[153]
MnO_2@Carbon fiber	$ZnCl_2$ and NH_4Cl	158 mAh·g^{-1} at 0.07 A·g^{-1}	–	-	[154]
MnO_2@Carbon paper	PVA/$ZnCl_2$/$MnSO_4$ gel	366.6 mAh·g^{-1} at 0.74 A·g^{-1}	504.9 Wh·kg^{-1}	83.7% after 300 at 1.11 A·g^{-1}	[155]

power densities in conjunction with excellent mechanical flexibility and long cycling life.

Transitional metal oxides such as nanostructured molybdenum oxides have been highlighted in their prospect in advanced electrochemical storage. To date, there are only a few published studies on the use of molybdenum oxides as ZIB electrodes. Lu et al. examined the electrochemical properties of orthorhombic MoO_3 nanowires as Zn storage electrodes, proving their potential in ZIBs as high-capacity cathodes [110]. To enhance the practicability of MoO_3 cathodes, different approaches have been taken to minimize the occurrence of instability caused by operating in an aqueous electrolyte. For example, a MoO_3 nanowire cathode operating with a quasi-solid electrolyte could deliver decent capacity retention over 70.4% after 400 cycles. This observation indicated that the quasi-solid electrolyte gave better performance than the aqueous electrolyte delivering capacity retention of only 27.1%. Furthermore, successful surface engineering of MoO_3 can be exploited as an alternative to quasi-solid electrolyte. Lu et al. [157] investigated fiber-shaped ZIBs based on the P-MoO_{3-x}@Al_2O_3 cathode. They concluded that Al_2O_3 coating could alleviate structure collapse or dissolution of MoO_3, resulting in better cyclic stability. In addition, the phosphorylation process could introduce oxygen vacancies and surface phosphate ions, thus giving MoO_3 rapid charge transport and surface reactivity.

Furthermore, Wang et al. developed a fiber-based ZIB via the synergistic interfacial design of the quinone-rich polydopamine (PDA) as organic redox-active cathodes and nanobinders on the carbon substrate [158]. Removing soluble monomers or oligomers and increasing the proportion of quinone groups were verified to be the key to improving the specific capacity and cycle stability. Besides, Zhang et al. explored the feasibility of poly(2,5-dihydroxy-1,4-benzoquinonyl sulfide) (PDBS) as a novel flexible organic cathode for Zn ion storage with elastic structural factors [159]. The malleable polymer chain structure could be arbitrarily rotated and bent for the facile Zn ion insertion, indicating the unique advantages of organic electrode materials in Zn ion storage. Furthermore, Liang et al. rationally designed an organic (ethylenediamine, EDA)-inorganic (vanadium oxide) hybrid nanoribbon cathodes for ultrahigh-rate and ultralong-life ZIBs [160]. It demonstrated that the embedded EDA could not only facilitate the Zn ion mobility in the V–O layered structure by increasing the layer spacing but also involved in Zn ion storage as a bidentate chelating ligand. This hybrid nanoribbon electrode delivered a high specific capacity (382.6 $mAh{\cdot}g^{-1}$ at 0.5 $A{\cdot}g^{-1}$), elevated voltage (0.82 V) and long-term cyclic durability (over 10,000 cycles at 5 $A{\cdot}g^{-1}$). All these results have profoundly demonstrated the great potential of organic material kind cathode and more extensive research is required.

Fiber-Based Materials as Anodes

Despite being a promising candidate for energy storage, Zn anode may suffer from quick loss of capacity during usage. The influencing factors could be a high degree of Zn dendrite formation, corrosion, hydrogen evolution, and passivation that have occurred on the electrode [161]. To address these issues, researchers have conducted extensive studies to exploit techniques for enhancing the performance of Zn anodes, including unique anode structures, optimal electrolyte compositions, new separator materials, and Zn anode/electrolyte interfacial modifications [162]. In terms of simplicity, efficiency, and operability, the interfacial modification strategy between electrode and electrolyte is therefore regarded as a better strategy. It can inhibit the generation of Zn dendrite and side reactions, which can improve the cycle life and charge–discharge performance of the Zn anode. For instance, a pasted Zn electrode could be manufactured from an aqueous mixture of Zn oxide, polytetrafluoroethylene, lead oxide, and cellulose fibers to inhibit the corrosion of the Zn anode induced by the pore plugging of a separator and suppress hydrogen evolution [125]. Cellulose fibers also showed great potential for enhancing wettability and mitigating the porosity changes of the anode. The result demonstrated the addition of 10% cellulose fibers to the pasted Zn electrode enhanced both cycle life and peak power drain capability [125]. Besides, the structures of current collectors also play an active role in the design of 3D Zn electrodes. Coating Zn on 3D fiber-based materials like porous conductive graphene foam [163], flexible carbon cloth [155], interwoven CNT paper [127], and nickel-titanium wire [153] have successfully minimized the dendrite formation on Zn anode. These studies also demonstrated that active materials in fiber-based structures had the potential to improve the rate capability and durability of ZIBs.

Fiber-Based Materials as Current Collectors

Current collectors are key components to collect electrons from electrodes and transport the electrons to the external circuit. Therefore, it is crucial for current collectors to possess rapid conductivity, good chemical and electrochemical stability, high mechanical strength, and decent adhesion to the active substance of the electrode. To achieve these requirements, conductive fiber-based materials such as carbon, metal, and conductive polymers are generally selected for flexible current collectors in ZIBs.

Carbon-Based Current Collectors

Carbon nanomaterials generally possess high electrical conductivity, light weight, good porosity and rough surfaces that facilitate high-quality mass loading for the battery and enhance surface adhesion to the electrode. 1D carbon fibers like CNT are often interwoven into porous networks or films for promoting active material loading and rapid electron transfer. Ma et al. suggested the fabrication of CNT fibers with a diameter ranging from 80 to 100 μm through direct dry-spinning for supporting the vertical growth of MnO_2 nanosheets [82]. Subsequently, a cable-type Zn/MnO_2 micro-battery was constructed with MnO_2@CNT and Zn wire, and this battery could be folded into arbitrary shapes without sacrificing electrochemical performance (Fig. 5a). Besides, Wang et al. used graphite fiber as a skeleton for Zn metal anode in hybrid aqueous ZIB to fabricate a self-supported Zn@GF (graphite felt) negative electrode [164]. The graphite felt ensured a dendrite-free cycling performance of ZIBs, profiting from a larger electroactive area for rapid transporting electrons and even faster Zn deposition.

2D carbon materials, for instance carbon cloth, are often utilized as a flexible current collector in sandwich-type flexible ZIBs or conductive substrates. Zhi et al. reported that a sandwich flexible quasi-solid ZIB (Zn/E-MoS_2) could be prepared by hydrothermal growth of active materials directly on the surface of carbon cloth to expand the interlayer-spacing of MoS_2, and Zn nanosheets were electrodeposited on the surface of carbon cloth as the negative electrode, and the electrodes were operated in a gel electrolyte [165]. As depicted in Fig. 5b, the Zn/E-MoS_2 battery showed excellent

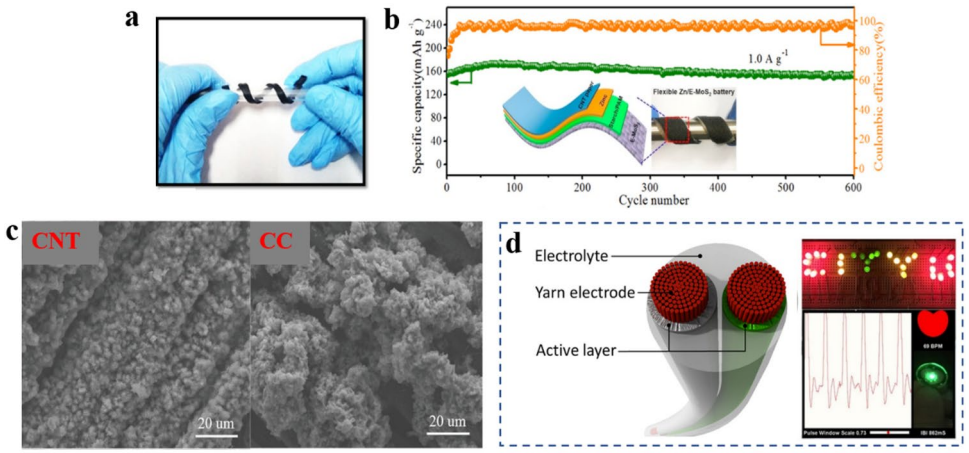

Fig. 5 **a** Flexibility of the Zn/MnO_2 cable battery; Reproduced with permission from ref [82], Copyright 2018, American Chemical Society. **b** Cycling stability of Zn/E-MoS_2 batteries at 1.0 $A{\cdot}g^{-1}$; Reproduced with permission from ref [165], Copyright 2018, Elsevier. **c** SEM images of CNT (**d**) and CC (**f**) after plating Zn with the capacity of 5 $mAh{\cdot}cm^{-2}$; Reproduced with permission from ref [169], Copyright 2019, Wiley–VCH. **d** Free-standing solid-state yarn battery powering LEDs (upper right), and a pulse sensor (bottom right); Reproduced with permission from ref [114], Copyright 2017, American Chemical Society

cycling stability for 500 cycles and maintained good electrochemical performance even under severe deformation conditions. Xia and Zhi et al. also reported their studies on sandwiched flexible Zn-MnO_2 batteries using carbon cloth as a flexible substrate [166, 167]. Both flexible batteries could deliver reliable working properties under various bending deformations.

Simple surface modification techniques can also be employed to enhance the electrochemical properties of carbon cloth. For example, Tong et al. reported the preparation of a Zn-MnO_2 flexible battery using nitrogen-doped carbon cloth as the collector [168]. Nitrogen-doped carbon cloth had a higher surface area, more active sites, and better conductivity, thus achieving uniform deposition of Zn and MnO_2. Moreover, Lu et al. proposed a flexible current collector by introducing the random CNT arrays on carbon cloth via the chemical vapor deposition method [169]. When compared to a pristine deposited Zn electrode, the 3D CNT framework on carbon cloth established a more uniformly distributed electric field for the dendrite-free Zn deposition process, as shown in Fig. 5c. This resulted in highly reversible Zn plating/stripping with high Coulombic efficiency with much less formation of Zn dendrites or other byproducts.

Metal-Based Current Collectors

Metal fibers with high conductivity and mechanical properties are suitable to be applied as flexible current collectors in ZIBs [113]. Zhi et al. found that stainless steel 316L could be spun at high temperatures to produce micron-sized filaments, which could then be drawn continuously using a twist-bundle drawing technique [114]. The as-drawn highly conductive long yarns were as flexible as cotton yarns owing to the intrinsic flexibility of micron-sized stainless-steel filaments. A nickel–cobalt (NiCo)//Zn wrist band battery was successfully prepared by uniformly electrodepositing Zn nanosheets and NiCo hydroxide nanosheets onto these conductive stainless-steel yarns, which served as an excellent fiber-based current collector, as shown in Fig. 5d. In addition, such conductive metallic yarns could be facilely woven by conventional weaving machine, which demonstrated a promising commercial potential for dual functions of wearability and energy storage.

Other studies also illustrated the use of common metal fibers for fabricating ZIBs. 3D fiber-based system was created by employing iron fibers as an anode collector that provided a consistent platform for supporting Zn efficiently [115]. Similarly, silver fibers with good electrical conductivity (7.4×10^4 $S{\cdot}m^{-1}$) and mechanical stability (38.39 cN/dtex) were adopted as an ideal flexible current collector [81]. A flexible all-solid fiber-based battery could therefore be constructed using the obtained fiber electrodes with a helix structure, which exhibited a promising prospect of wearable applications.

Conductive Polymer-Based Current Collectors

The electrochemical and lithe character of conductive polymers like PPy makes them a suitable candidate for producing flexible and wearable devices. In this regard, Li et al. developed a novel PPy/poly(3,4-ethylenedioxythiophene) polystyrene sulfonate (PEDOT:PSS) core-sheath fiber as ZIB cathode with an ultrahigh conductivity of 3700 $S{\cdot}cm^{-1}$[170]. The deposited PPy possessed a rough surface texture with

well-distributed nanogranules, which offered a large number of active sites and enhanced rapid ion diffusion kinetics. The assembled fiber-based ZIB delivered a high capacity of 162.3 mAh·g^{-1} at 0.08 A·g^{-1} and capacity retention up to 92.4% for 1,000 cycles with a Coulombic efficiency of around 100%. Besides, it demonstrated amazing integrability with high energy density applications, outstanding mechanical flexibility, and wide temperature resistance, proving its applicability in harsh environments.

The aforementioned fiber-based current collectors reported in earlier experiments were summarized in Table 4. It is notable that relevant studies are still extremely limited, and thus future investigation in this area is imperative. Nevertheless, it is anticipated that breakthroughs in high-performance ZIBs can be made based on the pioneering research indicated above.

Fiber-Based Materials as Separators and Gel Electrolytes

Separator significantly contributes to the total performance of ZIBs because it can isolate the cathode from the anode to prevent short circuits induced by electron transmission between electrodes and provide efficient pathways for carrier transmission. An ideal separator should possess sufficient pores, high mechanical strength, good ionic conductivity, and appropriate electrolyte wettability [171]. In addition, it is expected to modulate the Zn deposition process to further inhibit the formation of Zn dendrites. However, the performance of most commercial separators is far from satisfactory. Hence, modifications are required to improve their performance, and the development of new separator materials is also anticipated.

Ceramic-Based Separators

GF is one of the most often utilized separator materials for ZIBs in current studies, but the undesirable growth of Zn dendrite on it has retarded the development of ZIBs. To alleviate this issue, some studies have recently been focused on the modification of GF. For example, Wang et al. created GF@SM, a novel form of glass microfiber made with supramolecule (SM) [39]. Polar groups like amino, carbonyl, and triazine groups were prevalent in GF@SM. Those polar groups had favorable adsorption on Zn^{2+} ions, and thus hindered the buildup of Zn^{2+} ions and dendrites in the nearby area.

Besides, Sun et al. [171] designed a bifunctional separator by in situ growth of nitrogen-doped carbon (NC) on a pristine GF separator (Fig. 6a). NC/GF separator could effectively inhibit the formation and growth of Zn dendrite, resulting in stable charge/discharge cycles for more than 1,100 h under 1 mA·cm^{-2}/1 mAh·cm^{-2}. Zhang et al. discovered that GO-modified GF separator could stabilize Zn anode by promoting the prior formation of non-protruding crystal planes of Zn metal [172]. More notably, Sun et al.

Table 4 Comparisons of the electrochemical performance of the typical reported current collector materials for aqueous ZIBs

Electrode material	Current collector	Specific capacity	Energy/power densities	Cycling performance	Ref
Zn wire//MnO_2@CNT Fiber	CNT fiber	322 mAh·g^{-1} at 0.1 A·g^{-1}	437 Wh·kg^{-1}	85% retained after 100 cycles	[82]
Zn@GF// HQ-NaFe	Graphite felt	–	–	95% retained after 150 cycles at 100 mA·g^{-1}	[164]
Zn//MoS_2@CC	Carbon fiber cloth	202.6 mAh·g^{-1} at 0.1 A·g^{-1}	148.2 Wh·kg^{-1}	98.6% retained after 600 cycles at 0.1 A·g^{-1}	[165]
Zn@VMG //P-MnO_{2-x}@VMG	Carbon cloth	302.8 mAh·g^{-1} at 0.5 A·g^{-1}	369.5 Wh·kg^{-1}	90% retained after 1,000 cycles at 2 A·g^{-1}	[166]
Zn foil//MnO_2@N-CC	Carbon cloth	353 mAh·g^{-1} at 1 A·g^{-1}	440 Wh·kg^{-1}	93.6% after 1,000 cycles at 1 A·g^{-1}	[168]
Zn@CNT//MnO_2	CNT	300 mAh g^{-1} at 1 A·g^{-1}	126 Wh kg^{-1}	88.7% after 1,000 cycles at 20 mA·cm^{-2}	[169]
Zn//NCHO@Conductive Yarns	Stainless steel yarn	5 mAh·cm^{-3}	32.8 mW·cm^{-2}	60% retained after 1,000 cycles	[114]
Zn@IF//MnO_2	Iron fiber	–	–	78% retained after 200 cycles	[115]
eG//P-Zn@SFB	Silver fiber	32.56 mAh·cm^{-3} at 10 mA·cm^{-3}	36.04 mWh·cm^{-3}	76.5% after 1,000 cycles at 50 mA·cm^{-3}	[81]
Zn@CFs//PEDOT:PSS fiber	Carbon fiber	162.3 mAh·g^{-1} at 0.08 A·g^{-1}	210.1 Wh·kg^{-1}	92.4% after 1,000 cycles at 0.16 A· g^{-1}	[170]
Zn@CNT//MnO_2@CNT	CNT paper	306 mAh·g^{-1}	148.2 mW·cm^{-2}	97% retained after 1,000 cycles at 2,772 mA·g^{-1}	[127]

reported that the vertical graphene grown on the GF separator could homogenize the electric field and reduce the local current density, enabling impressively high rate capacities and durable cycle performance (93% over 5,000 cycles at 5 $A{\cdot}g^{-1}$) [173]. Although modification of GF separators has been confirmed to be efficient in improving the cycle performance, the high cost of modification procedures still constrains their commercial application.

Polymers-Based Separators

Natural Fiber-Based Separators Recent research works revealed that polymeric materials like cellulose could be an alternative to GF for the fabrication of separators. For instance, Wong et al. designed a cellulose-film (CF) separator with homogenous dense nanopores using cotton-derived cellulose materials, which endowed the separator with a high concentration of hydroxyl groups and high tensile modulus [124]. As shown in Fig. 6b, the CF separator (33.6 $kJ{\cdot}mol^{-1}$) demonstrated to have lower activation energy (E_a) than the GF separator (43.4 $kJ{\cdot}mol^{-1}$), indicating that the CF separator was effective in removing water sheath in $[Zn(H_2O)_6]^{2+}$ and enhanced Zn deposition kinetics. Furthermore, the CF separator could significantly improve the Zn stripping/plating reversibility by minimizing Zn dendrite growth and other unfavorable side reactions. Chen et al. proposed coating the Zn anode surface with cellulose fiber composite using a simple vacuum filtration process [174]. The intimate contact and high degree of compatibility between the cellulose-based separator and the electrode were essential for cell performance optimization. Such rational structural design substantially enhanced the electrochemical kinetics, and effectively addressed the challenges faced by the Zn foil anode.

Currently, functional cellulose separators can be constructed with the incorporation of other materials to increase the electrochemical performance of the Zn anode. By using an unusually stable crystal orientation operation in Zn^{2+} ion electrodeposition process, a cellulose/GO composite separator could facilitate the formation of a super stable dendritic free anode [52]. Since GO had outstanding Zn lattice compatibility, good stability, and a large specific surface area, this allowed the Zn deposited on the GO substrate to be compact, homogeneous, and nondendritic [175]. Besides, Cao et al. developed a ZrO_2/cellulose composite separator, which could promote the nucleation process, accelerate the ion diffusion kinetics, and also obviously undermines the side reactions and hydrogen evolution reaction of Zn anode (Fig. 6c) [53]. Additionally, Xue et al. modified a commercial CF separator by coating a layer of g-C_3N_4 nanosheets onto it, achieving enhanced electrochemical properties [176]. Therefore, different approaches may be taken to modify cellulose-based separators for high-performance ZIBs.

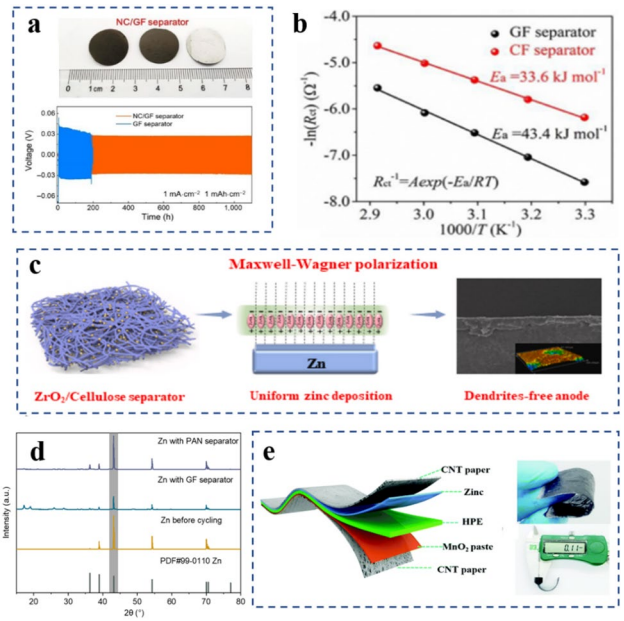

Fig. 6 **a** Long-term galvanostatic cycling of Zn//Zn symmetric cells at a current density of 1 $mA{\cdot}cm^{-2}$ and a capacity of 1 $mAh{\cdot}cm^{-2}$; Reproduced with permission from ref [171], Copyright 2021, Springer Nature. **b** Arrhenius curves and corresponding desolvation activation energy values of Zn//Zn cells with GF and CF separators; Reproduced with permission from ref [124], Copyright 2021, Elsevier. **c** Fabrication process of ZrO_2/cellulose composite separator and its advantages; Reproduced with permission from ref [53], Copyright 2021, Elsevier. **d** x-ray diffraction (XRD) pattern of the Zn electrode after 1,600 cycles at a current density of 1.766 $mA{\cdot}cm^{-2}$ with or without GF and PAN separator; Reproduced with permission from ref [177], Copyright 2021, Wiley–VCH. and **e** Schematic illustration of the structure of the solid-state ZIB and its thickness (0.11 mm); Reproduced with permission from ref [127], Copyright 2008, Royal Society of Chemistry

Synthetic Fiber-Based Separators

Polymeric fibrous membranes have the advantages of high mechanical flexibility, easy adaptation to strain, and high versatility in terms of customizing the various functional groups [178]. In the past few years, fibrous separators prepared by electrospinning technology have been widely used in the research of batteries because of their high porosity, superior ion migration ability, and variable functionalization. These are essential in achieving uniform distribution of electric charges on the electrode surface [179, 180]. Among them, PAN polymers have attracted great research interest due to their good chemical inertness, flame retardancy, and electrochemical stability in aqueous ZIBs. For instance, Liang et al. designed a 3D long-range ordered PAN nanofiber separator [177]. In addition to the uniform porous structure of nanofibers, the nitrogen atoms on the surface of the separator also contributed to the uniform distribution of

the ion flux and guided the cation transport through available N-Zn bonds. The Zn anode with a PAN separator demonstrated long-term stability and gave a dendrite-free deposition layer with a preferred (101) crystallographic orientation, as demonstrated in Fig. 6d.

Based on the electrospun PAN nanofiber, Zhi et al. further developed a high-performance hierarchical polymer electrolyte by crosslinking porous gelatin-g-PAM hydrogel in PAN fiber membrane pores [127]. This electrolyte exhibited high Zn ion conductivity and superior mechanical properties, enabling a wearable solid-state ZIB product with excellent flexibility and ultra-thin thickness (Fig. 6e). More notably, the solid-state ZIBs operating in polymer electrolytes can be a safer alternative to the conventional flexible LIBs operating in a liquid electrolyte, and it can also operate stably in a variety of harsh conditions. However, the ionic conductivity and electrochemical window of the polymer electrolytes still require substantial improvement before their practical usage in flexible ZIBs.

Conclusions and Outlook

Investigations on the high-performance ZIBs has become particularly important owing to their potential applications in grid energy storage systems, more environmentally benign manufacturing process, as well as the abundance of Zn resources. In addition, the increasing demands for novel wearable electronics and implantable medical kits have necessitated the development of ZIBs as a viable alternative to both traditional and flexible LIBs. Similar to flexible LIBs, the advancement of flexible ZIBs heavily relies on the pliability of the electrode materials and the battery constructions for achieving high performance and stability under mechanical deformation. It is worth noting that fiber-based materials have gained much attention in the development of advanced flexible ZIBs for wearable technology. Diverse morphologies, mechanical properties and electrochemical behaviors of fiber-based materials can efficiently boost the performance of ZIB electrodes. To attain the overall flexibility of ZIBs, pliable fiber-based materials like carbons, polymers, and their composites are commonly used to replace the materials of current collector, separator and binder used in traditional LIBs. However, pliable and layered active electrode materials, which are used in traditional LIBs, can generally be an ideal choice for flexible ZIBs with some exceptions showing performance lapses. Furthermore, polymeric materials may be applied as flexible solid-state electrolytes to replace traditional liquid electrolytes. It should be noted that lower ionic conductivity and narrower electrochemical window of some recently developed ZIB components still limit their practical usage in flexible ZIBs. Nevertheless, the progressive improvement of fiber-based ZIB components together with the recent breakthrough in flexible cathode materials have enhanced the electrochemical performance of ZIBs, bringing them a step closer to practical application.

It is important to address the existing shortcomings and challenges before the full application potential of fiber-based ZIBs can be realized in wearable electronics. The gravimetric and volumetric energy densities of ZIBs are generally less than that of commercialized batteries. These are evident challenges in preventing the complete implementation of ZIBs in the flexible wearable electronics industry. More specifically, ZIB capacity retention and cycle life are limited by repetitive mechanical bending deformations. The performance of ZIBs can likely be improved through material modification, material optimization, and advanced system architecture development. More so, inadequate studies on the performances of ZIBs in practical conditions, insufficient research about the integration and connection of ZIBs in wearable electronics, unresolved problems in automated production processes, and high battery preparation costs impede the advancement of ZIBs towards more practical uses. As a result, future ZIB research studies and development should concentrate on the following areas:

(a) Optimal design of ultra-flexible high-performance electrode materials

As flexible ZIBs need the ability to tolerate massive deformations, the electrode materials should meet stringent quality standards. With excellent versatility, high conductivity, outstanding mechanical quality and great chemical stability, carbon fiber-based materials have become one of the highlighted materials for the fabrication of various types of flexible electrodes. The diverse morphology range and intrinsic nature of these materials can synergize with different active ingredients to yield exceptional electrochemical performance in flexible ZIBs for meeting commercial standards.

(b) Optimization of solid, gel, and hybrid polymer electrolytes

The employment of solid and gel fiber-based electrolytes in ZIBs can efficiently resolve the leakage problem, caused by conventional liquid electrolytes. The use of hybrid or composite structures, such as inorganic–organic polymer electrolytes, offers another approach to improving ionic conductivity and electrochemical stability of the cell. Significant progress has been made in the development of these electrolytes, yet more effort is still needed to understand the unique ion transport mechanism. For designing polymer electrolytes in flexible ZIBs, materials with higher cation transport numbers, wider electrochemical windows, and lower operating temperatures are preferred. The

utilization of single-ion conducting polymers may also solve the undesirable contribution of anions to ionic conductivity.

(c) Construction of advanced battery architectures

More effort is needed in the construction of advanced fiber-based functional ZIB architectures in different dimensions with specific morphologies in the micro/nanoscale. These will enable diverse application possibilities for ZIB in various scenarios, expanding its practical usefulness in various energy storage fields. In addition, some studies have started to explore the all-in-one integrated configuration with a seamless interface, improving both mechanical and electrochemical performance. Moreover, green chemistry can be adopted to minimize the employment of harmful reagents, non-biodegradable active materials, and complicated production methods for manufacturing energy storage devices.

(d) Integration and connection considerations for wearable technology

The application of ZIB systems for wearable electronic applications may involve their integration onto or into substrates. The choice of integration methods requires consideration of the material nature, material structure, and construction of the whole device. This ensures that the ZIB system can withstand the damage risks during the integration process and retain its normal performance. The physical or chemical ways for connecting electrical devices with substrates and electronic devices should also guarantee sufficient flexibility under natural deformation, consistency in electrical contact, and feasibility of production under specific conditions.

(e) Ongoing advancements in ZIB systems for practical applications

From a practical point of view, washable and highly stable rechargeable ZIB systems can greatly boost the wearable application of this type of battery. Treatments including encapsulation or fabrication with waterproof materials can increase the tolerance of ZIBs to washing conditions. In addition, stable rechargeable ZIB systems can be operated efficiently alongside energy harvesting units. This supports the advancement of combining energy conversion and energy storage devices for acquiring self-powering wearable electronics. Besides, the human/textile interface design of fiber-based electronics can promote wear comfort.

(f) Scalability and automation for ZIB production

Although ZIBs have yet to gain significant commercial momentum in comparison to LIBs, their commercial potential is enormous. Extensive research has revealed that great outcomes of ZIB production can be achieved on a laboratory scale. Thus, these fundamental studies can support the investigation of large-scale automated methods for the cost-effective manufacturing of ZIBs, particularly the mass production of flexible electrodes, current collectors, separators and electrolytes for efficient battery assembly and battery integration. The fabrication of some fiber-based structures can be well supported by current textile manufacturing facilities, equipped with a sophisticated automatic production line. For some complicated morphologies, the fabrication may be feasible by template-assisted methods, 3D printing, laser technology or a hybrid approach integrating different manufacturing techniques.

Acknowledgements This work was financially supported by the Natural Science Foundation of Jiangsu Province (BK20210480) and Hong Kong Scholars Program (P0035017).

Declarations

Conflict of Interest The authors declare no conflict of interest.

References

1. Shi FY, Chen CH, Xu ZL. Recent advances on electrospun nanofiber materials for post-lithium ion batteries. *Adv Fiber Mater* **2021**;*3*:275–301.
2. Yan CY, Zhu P, Jia H, Du Z, Zhu JD, Orenstein R, Cheng H, Wu NQ, Dirican M, Zhang XW. Garnet-rich composite solid electrolytes for dendrite-free, high-rate, solid-state lithium-metal batteries. *Energy Stor Mater* **2020**;*26*:448–56.
3. Yang Y, Okonkwo EG, Huang GY, Xu SM, Sun W, He YH. On the sustainability of lithium ion battery industry-a review and perspective. *Energy Stor Mater* **2021**;*36*:186–212.
4. Yan CY, Zhu P, Jia H, Zhu JD, Selvan RK, Li Y, Dong X, Du Z, Angunawela I, Wu NQ, Dirican M, Zhang XW. High-performance 3D fiber network composite electrolyte enabled with Li-ion conducting nanofibers and amorphous PEO-based crosslinked polymer for ambient all-solid-state lithium-metal batteries. *Adv Fiber Mater* **2019**;*1*:46–60.
5. Li JW, Zhang XN, Lu YY, Linghu K, Wang C, Ma ZL, He XH. Electrospun fluorinated polyimide/polyvinylidene fluoride composite membranes with high thermal stability for lithium ion battery separator. *Adv Fiber Mater* **2022**;*4*:108–18.
6. Chan CY, Wang ZQ, Jia H, Ng PF, Chow L, Fei B. Recent advances of hydrogel electrolytes in flexible energy storage devices. *J Mater Chem A* **2021**;*9*:2043–69.
7. Wang ZQ, Huang WY, Hua JC, Wang YD, Yi HC, Zhao WG, Zhao QH, Jia H, Fei B, Pan F. An anionic-MOF-based bifunctional separator for regulating lithium deposition and suppressing polysulfides shuttle in Li-S batteries. *Small Methods* **2020**;*4*:2000082.
8. Jia H, Wang ZQ, Tawiah B, Wang YD, Chan CY, Fei B, Pan F. Recent advances in zinc anodes for high-performance aqueous Zn-ion batteries. *Nano Energy* **2020**;*70*:104523.
9. Jia H, Qiu MH, Lan CT, Liu HQ, Dirican M, Fu SH, Zhang XW. Advanced zinc anode with nitrogen-doping interface induced by plasma surface treatment. *Adv Sci* **2022**;*9*:2103952.
10. Jia H, Qiu MH, Tang CX, Liu HQ, Fu SH, Zhang XW. Nanoscale BN interface for ultra-stable and wide temperature range tolerable Zn anode. *Ecomat* **2022**;*4*:e12190.

11. Chao DL, Zhou WH, Xie FX, Ye C, Li H, Jaroniec M, Qiao SZ. Roadmap for advanced aqueous batteries: from design of materials to applications. *Sci Adv* **2020**;*6*:eaba4098.
12. Zhao XY, Liang XQ, Li Y, Chen QG, Chen MH. Challenges and design strategies for high performance aqueous zincion batteries. *Energy Stor Mater* **2021**;*42*:533–69.
13. Hu P, Zhu T, Wang XP, Wei XJ, Yan MY, Li JT, Luo W, Yang W, Zhang WC, Zhou L, Zhou ZQ, Mai LQ. Highly durable Na2V6O16·1.63H2O nanowire cathode for aqueous zinc-ion battery. *Nano Lett* **2018**;*18*:1758–63.
14. Jia H, Wang ZQ, Dirican M, Qiu S, Chan CY, Fu SH, Fei B, Zhang XW. A liquid metal assisted dendrite-free anode for high-performance Zn-ion batteries. *J Mater Chem A* **2021**;*9*:5597–605.
15. Wang ZQ, Dong LB, Huang WY, Jia H, Zhao QH, Wang YD, Fei B, Pan F. Simultaneously regulating uniform Zn^{2+} flux and electron conduction by MOF/rGO interlayers for high-performance Zn anodes. *Nano-Micro Lett* **2021**;*13*:73.
16. Yan MY, He P, Chen Y, Wang SY, Wei QL, Zhao KN, Xu X, An QY, Shuang Y, Shao YY, Mueller KT, Mai LQ, Liu J, Yang JH. Water-lubricated intercalation in $V_2O_5{\cdot}nH_2O$ for high-capacity and high-rate aqueous rechargeable zinc batteries. *Adv Mater* **2018**;*30*:1703725.
17. Zhao HN, Fu Q, Yang D, Sarapulova A, Pang Q, Meng Y, Wei LY, Ehrenberg HM, Wei YJ, Wang CZ, Chen G. In operando synchrotron studies of NH^{4+} preintercalated $V_2O_5{\cdot}nH_2O$ nanobelts as the cathode material for aqueous rechargeable zinc batteries. *ACS Nano* **2020**;*14*:11809–20.
18. Yang YQ, Tang Y, Fang GZ, Shan LT, Guo JS, Zhang WY, Wang C, Wang LB, Zhou J, Liang SQ. Li^+ intercalated $V_2O_5{\cdot}nH_2O$ with enlarged layer spacing and fast ion diffusion as an aqueous zinc-ion battery cathode. *Energy Environ Sci* **2018**;*11*:3157–62.
19. Wu J, Kuang Q, Zhang K, Feng JJ, Huang CM, Li JJ, Fan QH, Dong YZ, Zhao YM. Spinel $Zn_3V_3O_8$: a high-capacity zinc supplied cathode for aqueous Zn-ion batteries. *Energy Stor Mater* **2021**;*41*:297–309.
20. Liu YZ, Chi XW, Han Q, Du YX, Huang JQ, Liu Y, Yang JH. Alpha-MnO_2 nanofibers/carbon nanotubes hierarchically assembled microspheres: approaching practical applications of high-performance aqueous Zn-ion batteries. *J Power Sources* **2019**;*443*:227244.
21. Reddy ALM, Shaijumon MM, Gowda SR, Ajayan PM. Coaxial MnO_2/carbon nanotube array electrodes for high-performance lithium batteries. *Nano Lett* **2009**;*9*:1002–6.
22. Wang JJ, Wang JG, Liu HY, Wei CG, Kang FY. Zinc ion stabilized MnO_2 nanospheres for high capacity and long lifespan aqueous zinc-ion batteries. *J Mater Chem A* **2019**;*7*:13727–35.
23. Zhang LY, Chen L, Zhou XF, Liu ZP. Towards high-voltage aqueous metal-ion batteries beyond 1.5 V: the zinc/zinc hexacyanoferrate system. *Adv Energy Mater* **2015**;*5*:1400930.
24. Jiang BA, Huang T, Yang P, Xi X, Su YZ, Liu RL, Wu DQ. Solution-processed perylene diimide-ethylene diamine cathodes for aqueous zinc ion batteries. *J Colloid Interface Sci* **2021**;*598*:36–44.
25. Zhao Q, Huang WW, Luo ZQ, Liu LJ, Lu Y, Li YX, Li L, Hu JY, Ma H, Chen J. High-capacity aqueous zinc batteries using sustainable quinone electrodes. *Sci Adv* **2018**;*4*:eaao1761.
26. Chae MS, Heo JW, Kwak HH, Lee H, Hong ST. Organic electrolyte-based rechargeable zinc-ion batteries using potassium nickel hexacyanoferrate as a cathode material. *J Power Sources* **2017**;*337*:204–11.
27. Tang BY, Shan LT, Liang SQ, Zhou J. Issues and opportunities facing aqueous zinc-ion batteries. *Energy Environ Sci* **2019**;*12*:3288–304.
28. Song M, Tan H, Chao DL, Fan HJ. Recent advances in Zn-ion batteries. *Adv Funct Mater* **2018**;*28*:1802564.
29. Deng WJ, Li ZG, Ye YK, Zhou ZQ, Li YB, Zhang M, Yuan XR, Hu J, Zhao WG, Huang ZY, Li C, Chen HB, Zheng JX, Li R. Zn^{2+} induced phase transformation of $K_2MnFe(CN)_6$ boosts highly stable zinc-ion storage. *Adv Energy Mater* **2021**;*11*:2003639.
30. Fang GZ, Zhou J, Pan AQ, Liang SQ. Recent advances in aqueous zinc-ion batteries. *ACS Energy Lett* **2018**;*3*:2480–501.
31. Li HF, Xu CJ, Han CP, Chen YY, Wei CG, Li BH, Kang FY. Enhancement on cycle performance of Zn anodes by activated carbon modification for neutral rechargeable zinc ion batteries. *J Electrochem Soc* **2015**;*162*:A1439–44.
32. Li CP, Xie XS, Liang SQ, Zhou J. Issues and future perspective on zinc metal anode for rechargeable aqueous zinc-ion batteries. *Energy Environ Mater* **2020**;*3*:146–59.
33. Liu HQ, Qiu MH, Tang CX, Xu JL, Jia H. Enhance interfacial deposition kinetics to achieve dendrite-free zinc anodes by graphene oxide modified boron nitride nanosheets. *Electrochim Acta* **2022**;*405*:139776.
34. Yang HX, Cao YL, Ai XP, Xiao LF. Improved discharge capacity and suppressed surface passivation of zinc anode in dilute alkaline solution using surfactant additives. *J Power Sources* **2004**;*128*:97–101.
35. Guo LB, Guo H, Huang HL, Tao S, Cheng YH. Inhibition of zinc dendrites in zinc-based flow batteries. *Front Chem* **2020**;*8*:557.
36. Li HF, Liu ZX, Liang GJ, Huang Y, Huan Y, Zhu MS, Pei ZX, Xue Q, Tang ZJ, Wang YK, Li BH, Zhi CY. Waterproof and tailorable elastic rechargeable yarn zinc ion batteries by a cross-linked polyacrylamide electrolyte. *ACS Nano* **2018**;*12*:3140–8.
37. Qiu MH, Wang D, Tawiah B, Jia H, Fei B, Fu SH. Constructing PEDOT:PSS/graphene sheet nanofluidic channels to achieve dendrite-free Zn anode. *Compos B Eng* **2021**;*215*:108798.
38. Qiu MH, Liu HQ, Tawiah B, Jia H, Fu SH. Zwitterionic triple-network hydrogel electrolyte for advanced flexible zinc ion batteries. *Compos Commun* **2021**;*28*:100942.
39. Liu TC, Hong J, Wang JL, Xu Y, Wang Y. Uniform distribution of zinc ions achieved by functional supramolecules for stable zinc metal anode with long cycling lifespan. *Energy Stor Mater* **2022**;*45*:1074–83.
40. Nan D, Wang JG, Huang ZH, Wang L, Shen WC, Kang FY. Highly porous carbon nanofibers from electrospun polyimide/SiO_2 hybrids as an improved anode for lithium-ion batteries. *Electrochem Commun* **2013**;*34*:52–5.
41. Pampal ES, Stojanovska E, Simon B, Kilic A. A review of nanofibrous structures in lithium ion batteries. *J Power Sources* **2015**;*300*:199–215.
42. Xiong J, Chen J, Lee PS. Functional fibers and fabrics for soft robotics, wearables, and human-robot interface. *Adv Mater* **2021**;*33*:2002640.
43. Yu DS, Zhai SL, Jiang WC, Goh KL, Wei L, Chen XD, Jiang RR, Chen Y. Transforming pristine carbon fiber tows into high performance solid-state fiber supercapacitors. *Adv Mater* **2015**;*27*:4895–901.
44. Lu XH, Yu MH, Wang GM, Tong YX, Li Y. Flexible solid-state supercapacitors: design, fabrication and applications. *Energy Environ Sci* **2014**;*7*:2160–81.
45. Zhang Y, Zhao Y, Ren J, Weng W, Peng HS. Advances in wearable fiber-shaped lithium-ion batteries. *Adv Mater* **2016**;*28*:4524–31.
46. Zhang XW, Ji LW, Toprakci O, Liang YZ, Alcoutlabi M. Electrospun nanofiber-based anodes, cathodes, and separators for advanced lithium-ion batteries. *Polym Rev (Philadelphia, PA, U. S.)* **2011**;*51*:239–64.
47. Lu LJ, Hu YJ, Dai K. The advance of fiber-shaped lithium ion batteries. *Mater Today Chem* **2017**;*5*:24–33.

48. Chen XY, Wang LB, Li H, Cheng FY, Chen J. Porous V_2O_5 nanofibers as cathode materials for rechargeable aqueous zinc-ion batteries. *J Energy Chem* **2019**;*38*:20–5.
49. Volkov AI, Sharlaev AS, Berezina OY, Tolstopjatova EG, Fu L, Kondratiev VV. Electrospun V_2O_5 nanofibers as high-capacity cathode materials for zinc-ion batteries. *Mater Lett* **2022**;*308*:131212.
50. Zhang HB, Yao ZD, Lan DW, Liu YY, Ma LT, Cui JL. N-doped carbon/V_2O_3 microfibers as high-rate and ultralong-life cathode for rechargeable aqueous zinc-ion batteries. *J Alloys Compd* **2021**;*861*:158560.
51. Niu T, Li JB, Qi YL, Huang XB, Ren YR. Preparation and electrochemical properties of alpha-MnO_2/rGO-PPy composite as cathode material for zinc-ion battery. *J Mater Sci* **2021**;*56*:16582–90.
52. Cao J, Zhang DD, Gu C, Wang X, Wang SM, Zhang XY, Qin JQ, Wu ZS. Manipulating crystallographic orientation of zinc deposition for dendrite-free zinc ion batteries. *Adv Energy Mater* **2021**;*11*:2101299.
53. Cao J, Zhang DD, Gu C, Zhang XY, Okhawilai M, Wang SM, Han JT, Qin JQ, Huang YH. Modulating Zn deposition via ceramic-cellulose separator with interfacial polarization effect for durable zinc anode. *Nano Energy* **2021**;*89*:106322.
54. Li C, Li P, Yang S, Zhi CY. Recently advances in flexible zinc ion batteries. *J Semicond* **2021**;*42*:101603.
55. Wang YC, Jiang GS, Zhang Z, Chen HC, Li YT, Kong DB, Qin X, Li YY, Zhang XH, Wang H. Cable-Like V_2O_5 decorated carbon cloth as a high-capacity cathode for flexible zinc ion batteries. *Energy Technol* **2022**;*10*:2101170.
56. Zeng W, Shu L, Li Q, Chen S, Wang F, Tao XM. Fiber-based wearable electronics: a review of materials, fabrication, devices, and applications. *Adv Mater* **2014**;*26*:5310–36.
57. Shi QW, Sun JQ, Hou CY, Li YG, Zhang QH, Wang HZ. Advanced functional fiber and smart textile. *Adv Fiber Mater* **2019**;*1*:3–31.
58. Yang SN, Cheng Y, Xiao X, Pang H. Development and application of carbon fiber in batteries. *Chem Eng J* **2020**;*384*:123294.
59. Jia H, Dirican M, Chen C, Zhu JD, Zhu P, Yan CY, Li Y, Dong X, Guo JS, Zhang XW. Reduced graphene oxide-incorporated SnSb@CNF composites as anodes for high-performance sodium-ion batteries. *ACS Appl Mater Interfaces* **2018**;*10*:9696–703.
60. Jia H, Dirican M, Sun N, Chen C, Zhu P, Yan CY, Dong X, Du Z, Guo JS, Karaduman Y, Wang JS, Tang FC, Tao JS, Zhang XW. SnS hollow Nanofibers as anode materials for sodium-ion batteries with high capacity and ultra-long cycling stability. *Chem Commun* **2019**;*55*:505–8.
61. Wu LS, Dong YF. Recent progress of carbon nanomaterials for high-performance cathodes and anodes in aqueous zinc ion batteries. *Energy Stor Mater* **2021**;*41*:715–37.
62. Park SK, Dose WM, Boruah BD, De Volder M. In situ and operando analyses of reaction mechanisms in vanadium oxides for Li-, Na-, Zn-, and Mg-ions batteries. *Adv Mater Technol* **2022**;*7*:2100799.
63. Liu XY, Ma LW, Du YH, Lu QQ, Yang AK, Wang XY. Vanadium pentoxide nanofibers/carbon nanotubes hybrid film for high-performance aqueous zinc-ion batteries. *Nanomaterials* **2021**;*11*:1054.
64. Tang H, Jiang M, Ren E, Zhang Y, Lai X, Cui C, Jiang S, Zhou M, Qin Q, Guo R. Integrate electrical conductivity and Li^+ ion mobility into hierarchical heterostructure Ti_3C_2@CoO/ZnO composites toward high-performance lithium ion storage. *Energy* **2020**;*212*:118696.
65. Liu ZX, Mo FN, Li HF, Zhu MS, Wang ZF, Liang GJ, Zhi CY. Advances in flexible and wearable energy-storage textiles. *Small Methods* **2018**;*2*:1800124.
66. Liao M, Ye L, Zhang Y, Chen TQ, Peng HS. The recent advance in fiber-shaped energy storage devices. *Adv Electron Mater* **2019**;*5*:1800456.
67. Zhang L, Liu WX, Shi WH, Xu XL, Mao J, Li P, Ye CZ, Yin RL, Ye SF, Liu XY, Cao XH, Gao C. Boosting lithium storage properties of MOF derivatives through a wet-spinning assembled fiber strategy. *Chem-A Eur J* **2018**;*24*:13792–9.
68. Song WJ, Lee S, Song G, Son HB, Han DY, Jeong I, Bang Y, Park S. Recent progress in aqueous based flexible energy storage devices. *Energy Stor Mater* **2020**;*30*:260–86.
69. Chen D, Jiang K, Huang TT, Shen GZ. Recent advances in fiber supercapacitors: materials, device configurations, and applications. *Adv Mater* **2020**;*32*:1901806.
70. Kim H, Pyun KR, Lee MT, Lee HB, Ko SH. Recent advances in sustainable wearable energy devices with nanoscale materials and macroscale structures. *Adv Funct Mater* **2022**;*32*:2110535.
71. Lv T, Yao Y, Li N, Chen T. Wearable fiber-shaped energy conversion and storage devices based on aligned carbon nanotubes. *Nano Today* **2016**;*11*:644–60.
72. Pu J, Cao QH, Gao Y, Yang J, Cai DM, Chen X, Tang XW, Fu GW, Pan ZH, Guan C. Ultrafast-charging quasi-solid-state fiber-shaped zinc-ion hybrid supercapacitors with superior flexibility. *J Mater Chem A* **2021**;*9*:17292–9.
73. Jia H, Zhu JJ, Debeli DK, Li ZL, Guo JS. Solar thermal energy harvesting properties of spacer fabric composite used for transparent insulation materials. *Sol Energy Mater Sol Cells* **2018**;*174*:140–5.
74. Jia H, Zhu JJ, Li ZL, Cheng XM, Guo JS. Design and optimization of a photo-thermal energy conversion model based on polar bear hair. *Sol Energy Mater Sol Cells* **2017**;*159*:345–51.
75. Wang HM, Zhang S, Deng C. In situ encapsulating metal oxides into core-shell hierarchical hybrid fibers for flexible zinc-ion batteries toward high durability and ultrafast capability for wearable applications. *ACS Appl Mater Interfaces* **2019**;*11*:35796–808.
76. Zhang QC, Li CW, Li QL, Pan ZH, Sun J, Zhou ZY, He B, Man P, Xie LY, Kang LX, Wang XN, Yang J, Zhang T, Shum PP, Li QW, Yao YG, Wei L. Flexible and high-voltage coaxial-fiber aqueous rechargeable zinc-ion battery. *Nano Lett* **2019**;*19*:4035–42.
77. Hao YA, Hu F, Chen Y, Wang YH, Xue JJ, Yang SY, Peng SJ. Recent progress of electrospun nanofibers for zinc-air batteries. *Adv Fiber Mater* **2022**;*4*:185–202.
78. Huang A, Ma Y, Peng J, Li L, Chou SI, Ramakrishna S, Peng S. Tailoring the structure of silicon-based materials for lithium-ion batteries via electrospinning technology. *eScience* **2021**;*1*:141–62.
79. Li CP, Qiu M, Li RL, Li X, Wang MX, He JB, Lin GG, Xiao LR, Qian QR, Chen QH, Wu JX, Li XY, Mai YW, Chen YM. Electrospinning engineering enables high-performance sodium-ion batteries. *Adv Fiber Mater* **2022**;*4*:43–65.
80. Peng SJ, Li LL, Hu YX, Srinivasan M, Cheng FY, Chen J, Ramakrishna S. Fabrication of spinel one-dimensional architectures by single-spinneret electrospinning for energy storage applications. *ACS Nano* **2015**;*9*:1945–54.
81. Li M, Li ZQ, Ye XR, Zhang XJ, Qu LJ, Tian MW. Tendril-inspired 900% ultrastretching fiber-based Zn-ion batteries for wearable energy textiles. *ACS Appl Mater Interfaces* **2021**;*13*:17110–7.
82. Wang K, Zhang XH, Hang JW, Zhang X, Sun XZ, Li C, Liu WH, Li QW, Ma YW. High-performance cable-type flexible rechargeable Zn battery based on MnO_2@CNT fiber microelectrode. *ACS Appl Mater Interfaces* **2018**;*10*:24573–82.
83. Wang YY, Li ZG, Zhang P, Pan Y, Zhang Y, Cai Q, Silva SRP, Liu J, Zhang GX, Sun XM, Yan ZF. Flexible carbon nanofiber film with diatomic Fe-Co sites for efficient oxygen reduction and evolution reactions in wearable zinc-air batteries. *Nano Energy* **2021**;*87*:106147.

84. Mathew V, Sambandam B, Kim S, Kim S, Park S, Lee S, Alfaruqi MH, Soundharrajan V, Islam S, Putro DY, Hwang JY, Sun YK, Kim J. Manganese and vanadium oxide cathodes for aqueous rechargeable zinc-ion batteries: a focused view on performance, mechanism, and developments. *ACS Energy Lett* **2020**;*5*:2376–400.
85. Liu WB, Dong LB, Jiang BZ, Huang YF, Wang XL, Xu CJ, Kang Z, Mou J, Kang FY. Layered vanadium oxides with proton and zinc ion insertion for zinc ion batteries. *Electrochim Acta* **2019**. https://doi.org/10.1016/j.electacta.2019.134565 .
86. Chen D, Rui XH, Zhang Q, Geng HB, Gan LY, Zhang W, Li CC, Huang SM, Yu Y. Persistent zinc-ion storage in mass-produced V_2O_5 architecture. *Nano Energy* **2019**;*60*:171–8.
87. Yang D, Tan HT, Rui XH, Yu Y. Electrode materials for rechargeable zinc-ion and zinc-air batteries: current status and future perspectives. *Electrochem Energy Rev* **2019**;*2*:395–427.
88. Sambandam B, Soundharrajan V, Kim S, Alfaruqi MH, Jo J, Kim S, Mathew V, Sun YK, Kim J. Aqueous rechargeable Zn-ion batteries: an imperishable and high-energy $Zn_2V_2O_7$ nanowire cathode through intercalation regulation. *J Mater Chem A* **2018**;*6*:3850–6.
89. Li YW, Xu P, Jiang JQ, Yao JH, Huang B, Yang JW. Facile synthesis of ultra-large V_2O_5 xerogel flakes and its application as a cathode material for aqueous Zn-ion batteries. *Mater Today Commun* **2021**;*26*:101849.
90. Liu YY, Li Q, Ma KX, Yang GZ, Wang CX. Graphene oxide wrapped CuV_2O_6 nanobelts as high-capacity and long-life cathode materials of aqueous zinc-ion batteries. *ACS Nano* **2019**;*13*:12081–9.
91. Li YK, Huang ZM, Kalambate PK, Zhong Y, Huang ZM, Xie ML, Shen Y, Huang YH. V_2O_5 nanopaper as a cathode, aterial with high capacity and long cycle life for rechargeable aqueous zinc-ion battery. *Nano Energy* **2019**;*60*:752–9.
92. Mao FF, Li YW, Zou ZG, Huang B, Yang JW, Yao JH. Zn^{2+} storage performance and structural change of orthorhombic V_2O_5 nanowires as the cathode material for rechargeable aqueous zinc-ion batteries. *Electrochim Acta* **2021**;*397*:139255.
93. Pang Q, Sun CL, Yu YH, Zhao KN, Zhang ZY, Voyles PM, Chen G, Wei YJ, Wang XD. $H_2V_3O_8$ nanowire/graphene electrodes for aqueous rechargeable zinc ion batteries with high rate capability and large capacity. *Adv Energy Mater* **2018**;*8*:1800144.
94. Lin YT, Zhou FS, Chen M, Zhang S, Deng C. Building defect-rich oxide nanowires@graphene coaxial scrolls to boost high-rate capability, cycling durability and energy density for flexible Zn-ion batteries. *Chem Eng J* **2020**;*396*:125259.
95. Yu X, Hu F, Cui FH, Zhao J, Guan C, Zhu K. The displacement reaction mechanism of the CuV_2O_6 nanowire cathode for rechargeable aqueous zinc ion batteries. *Dalton Trans* **2020**;*49*:1048–55.
96. Cao HL, Peng C, Zheng ZY, Lan ZY, Pan QY, Nielsen UG, Norby P, Xiao XX, Mossin S. Orientation effect of zinc vanadate cathode on zinc ion storage performance. *Electrochim Acta* **2021**;*388*:138646.
97. Pan HL, Shao YY, Yan PF, Cheng YW, Han KS, Nie ZM, Wang CM, Yang JH, Li XL, Bhattacharya P, Mueller KT, Liu J. Reversible aqueous zinc/manganese oxide energy storage from conversion reactions. *Nat Energy* **2016**;*1*:16039.
98. De Juan-Corpuz LM, Corpuz RD, Somwangthanaroj A, Nguyen MT, Yonezawa T, Ma JM, Kheawhom S. Binder-free centimeter-long V_2O_5 nanofibers on carbon cloth as cathode material for zinc-ion batteries. *Energies* **2020**;*13*:31.
99. Ding JW, Du ZG, Gu LQ, Li B, Wang LZ, Wang SW, Gong YJ, Yang SB. Ultrafast Zn^{2+} intercalation and deintercalation in vanadium dioxide. *Adv Mater* **2018**;*30*:1800762.
100. Chen ZY, Hu JG, Liu SJ, Hou HS, Zou GQ, Deng WT, Ji XB. Dual defects boosting zinc ion storage of hierarchical vanadium oxide fibers. *Chem Eng J* **2021**;*404*:126536.
101. Zhang N, Cheng FY, Liu JX, Wang LB, Long XH, Liu XS, Li FJ, Chen J. Rechargeable aqueous zinc-manganese dioxide batteries with high energy and power densities. *Nat Commun* **2017**;*8*:405.
102. Sun W, Wang F, Hou SY, Yang CY, Fan XL, Ma ZH, Gao T, Han FD, Hu RZ, Zhu M, Wang CS. Zn/MnO_2 battery chemistry with H^+ and Zn^{2+} coinsertion. *J Am Chem Soc* **2017**;*139*:9775–8.
103. Alfaruqi MH, Mathew V, Gim J, Kim S, Song J, Baboo JP, Choi SH, Kim J. Electrochemically induced structural transformation in a gamma-MnO_2 cathode of a high capacity zinc-ion battery system. *Chem Mater* **2015**;*27*:3609–20.
104. Alfaruqi MH, Gim J, Kim S, Song J, Pham DT, Jo J, Xiu Z, Mathew V, Kim J. A layered delta-MnO_2 nanoflake cathode with high zinc-storage capacities for eco-friendly battery applications. *Electrochem Commun* **2015**;*60*:121–5.
105. Subjalearndee N, He NF, Cheng H, Tesatchabut P, Eiamlamai P, Limthongkul P, Intasanta V, Gao W, Zhang XW. Gamma((γ))-MnO_2/rGO fibered cathode fabrication from wet spinning and dip coating techniques for cable-shaped Zn-ion batteries. *Adv Fiber Mater* **2022**;*4*:457–74.
106. Wu MS, Guo ZS, Jow JJ. Highly regulated electrodeposition of needle-like manganese oxide nanofibers on carbon fiber fabric for electrochemical capacitors. *J Phys Chem C* **2010**;*114*:21861–7.
107. Chen JY, Zhou Y, Islam MS, Cheng XY, Brown SA, Han ZJ, Rider AN, Wang CH. Carbon fiber reinforced Zn-MnO_2 structural composite batteries. *Compos Sci Technol* **2021**;*209*:108787.
108. Song X, Wang HR, Li ZN, Du CF, Guo RS. A review of MnO_2 composites incorporated with conductive materials for energy storage. *Chem Rec* **2022**. https://doi.org/10.1002/tcr.202200118 .
109. Mai LQ, Hu B, Chen W, Qi YY, Lao CS, Yang RS, Dai Y, Wang ZL. Lithiated MoO_3 nanobelts with greatly improved performance for lithium batteries. *Adv Mater* **2007**;*19*:3712–6.
110. He XJ, Zhang HZ, Zhao XY, Zhang P, Chen MH, Zheng ZK, Han ZJ, Zhu TS, Tong YX, Lu XH. Stabilized molybdenum trioxide nanowires as novel ultrahigh-capacity cathode for rechargeable zinc ion battery. *Adv Sci* **2019**;*6*:1900151.
111. Murugesan D, Prakash S, Ponpandian N, Manisankar P, Viswanathan C. Two dimensional α-MoO_3 nanosheets decorated carbon cloth electrodes for high-performance supercapacitors. *Colloids Surf Physicochem Eng Aspects* **2019**;*569*:137–44.
112. Meng W, Xia YL, Ma CG, Du XS. Electrodeposited polyaniline nanofibers and moo_3 nanobelts for high-performance asymmetric supercapacitor with redox active electrolyte. *Polymers* **2020**;*12*:2303.
113. Huang Y, Hu H, Huang Y, Zhu MS, Meng WJ, Liu C, Pei ZX, Hao CL, Wang ZK, Zhi CY. From industrially weavable and knittable highly conductive yarns to large wearable energy storage textiles. *ACS Nano* **2015**;*9*:4766–75.
114. Huang Y, Ip WS, Lau YY, Sun JF, Zeng J, Yeung NSS, Ng WS, Li HF, Pei ZX, Xue Q, Wang YK, Yu J, Hu H, Zhi CY. Weavable, conductive yarn-based NiCo//Zn textile battery with high energy density and rate capability. *ACS Nano* **2017**;*11*:8953–61.
115. Khezri R, Jirasattayaporn K, Abbasi A, Maiyalagan T, Mohamad AA, Kheawhom S. Three-dimensional fibrous iron as anode current collector for rechargeable zinc-air batteries. *Energies* **2020**;*13*:1429.
116. Ye L, Hong Y, Liao M, Wang BJ, Wei DC, Peng HS, Ye L, Hong Y, Liao M, Wang B, Wei D, Peng H. Recent advances in flexible fiber-shaped metal-air batteries. *Energy Stor Mater* **2020**;*28*:364–74.
117. Tang H, Jiang M, Zhang Y, Lai X, Cui C, Xiao H, Jiang S, Ren E, Qin Q, Guo R. CNTs anchored on defective bimetal oxide $NiCoO_{2-x}$ microspheres for high-performance lithium-ion battery anode. *Electrochim Acta* **2020**;*354*:136760.

118. Tang H, Guo RH, Jiang MJ, Zhang Y, Lai XX, Cui C, Xiao HY, Jiang SX, Ren EH, Qin Q. Construction of Ti_3C_2 MXene@C@SnS with layered rock rtratum rtructure for high-performance lithium storage. *J Power Sources* **2020**;*462*:228152.
119. He B, Zhou ZY, Man P, Zhang QC, Li CW, Xie LY, Wang XN, Li QL, Yao YG. V_2O_5 nanosheets supported on 3D N-doped carbon nanowall arrays as an advanced cathode for high energy and high power fiber-shaped zinc-ion batteries. *J Mater Chem A* **2019**;*7*:12979–86.
120. Zhang XS, Pei ZX, Wang CJ, Yuan ZW, Wei L, Pan YQ, Mahmood A, Shao Q, Chen Y. Flexible zinc-ion hybrid fiber capacitors with ultrahigh energy density and long cycling life for wearable electronics. *Small* **2019**;*15*:1903817.
121. Qin Y, Liu P, Zhang Q, Wang Q, Sun D, Tang YG, Ren Y, Wang HY. Advanced filter membrane separator for aqueous zinc-ion batteries. *Small* **2020**;*16*:2003106.
122. Duay J, Keny M, Lambert TN. Evaluation of a ceramic separator for use in rechargeable alkaline Zn/MnO_2 batteries. *J Power Sources* **2018**;*395*:430–8.
123. Wang ZH, Lee YH, Kim SW, Seo JY, Lee SY, Nyholm L. Why cellulose-based electrochemical energy storage devices? *Adv Mater* **2021**;*33*:2000892.
124. Zhou WJ, Chen MF, Tian QH, Chen JZ, Xu XW, Wong CP. Cotton-derived cellulose film as a dendrite-inhibiting separator to stabilize the zinc metal anode of aqueous zinc ion batteries. *Energy Stor Mater* **2022**;*44*:57–65.
125. Muller S, Holzer F, Haas O. Optimized zinc electrode for the rechargeable zinc-air battery. *J Appl Electrochem* **1998**;*28*:895–8.
126. He GJ, Liu YY, Gray DE, Othon J. Conductive polymer composites cathodes for rechargeable aqueous Zn-ion batteries: a mini-review. *Compos Commun* **2021**;*27*:100882.
127. Li HF, Han CP, Huang Y, Huang Y, Zhu MS, Pei ZX, Xue Q, Wang ZF, Liu ZX, Tang ZJ, Wang YK, Kang FY, Li BH, Zhi CY. An extremely safe and wearable solid-state zinc ion battery based on a hierarchical structured polymer electrolyte. *Energy Environ Sci* **2018**;*11*:941–51.
128. Zhang SQ, Long ST, Li H, Xu Q. A high-capacity organic cathode based on active n atoms for aqueous zinc-ion batteries. *Chem Eng J* **2020**;*400*:125898.
129. Yoo G, Pyo S, Gong YJ, Cho J, Kim H, Kim YS, Yoo J. Highly reliable quinone-based cathodes and cellulose nanofiber separators: toward eco-friendly organic lithium batteries. *Cellulose* **2020**;*27*:6707–17.
130. Li Y, Zhu JD, Cheng H, Li GQ, Cho HJ, Jiang MJ, Gao Q, Zhang XW. Developments of advanced electrospinning techniques: a critical review. *Adv Mater Technol* **2021**;*6*:2100410.
131. Zhong HL, Huang J, Wu J, Du JH. Electrospinning nanofibers to 1D, 2D, and 3D scaffolds and their biomedical applications. *Nano Res* **2022**;*15*:787–804.
132. Ashraf R, Sofi HS, Malik A, Beigh MA, Hamid R, Sheikh FA. Recent trends in the fabrication of starch nanofibers: electrospinning and non-electrospinning routes and their applications in biotechnology. *Appl Biochem Biotechnol* **2019**;*187*:47–74.
133. Li B, Ge XM, Goh FWT, Hor TSA, Geng DS, Du GJ, Liu ZL, Zhang J, Liu XG, Zong Y. Co_3O_4 nanoparticles decorated carbon nanofiber mat as binder-free air-cathode for high performance rechargeable zinc-air batteries. *Nanoscale* **2015**;*7*:1830–8.
134. Kim J, Lee SH, Park C, Kim HS, Park JH, Chung KY, Ahn H. Controlling vanadate nanofiber interlayer via intercalation with conducting polymers: cathode material design for rechargeable aqueous zinc ion batteries. *Adv Funct Mater* **2021**;*31*:2100005.
135. Kang Z, Wu CL, Dong LB, Liu WB, Mou J, Zhang JW, Chang ZW, Jiang BZ, Wang GX, Kang FY, Xu CJ. 3D porous copper skeleton supported zinc anode toward high capacity and long cycle life zinc ion batteries. *ACS Sustain Chem Eng* **2019**;*7*:3364–71.
136. Yang G, Park SJ. Conventional and microwave hydrothermal synthesis and application of functional materials: a review. *Materials* **2019**;*12*:1177.
137. Pu J, Shen ZH, Zhong CL, Zhou QW, Liu JY, Zhu J, Zhang HG. Electrodeposition technologies for Li-based batteries: new frontiers of energy storage. *Adv Mater* **2020**;*32*:1903808.
138. Ahmad R, Wolfbeis OS, Hahn YB, Alshareef HN, Torsi L, Salama KN. Deposition of nanomaterials: a crucial step in biosensor fabrication. *Mater Today Commun* **2018**;*17*:289–321.
139. Indra A, Song T, Paik U. Metal organic framework derived materials: progress and prospects for the energy conversion and storage. *Adv Mater* **2018**;*30*:1705146.
140. Kundu D, Adams BD, Duffort V, Vajargah SH, Nazar LF. A high-capacity and long-life aqueous rechargeable zinc battery using a metal oxide intercalation cathode. *Nat Energy* **2016**;*1*:16119.
141. Li G, Yang Z, Jiang Y, Jin C, Huang W, Ding X, Huang Y. Towards polyvalent ion batteries: a zinc-ion battery based on NASICON structured $Na_3V_2(PO_4)_3$. *Nano Energy* **2016**;*25*:211–7.
142. Cai YS, Liu F, Luo ZG, Fang GZ, Zhou J, Pan AQ, Liang SQ. Pilotaxitic $Na_{1.1}V_3O_{7.9}$ nanoribbons/graphene as high-performance sodium ion battery and aqueous zinc ion battery cathode. *Energy Stor Mater* **2018**;*13*:168–74.
143. Xia C, Guo J, Lei YJ, Liang HF, Zhao C, Alshareef HN. Rechargeable aqueous zinc-ion battery based on porous framework zinc pyrovanadate intercalation cathode. *Adv Mater* **2018**;*30*:1705580.
144. Ni JF, Li L. Self-supported 3D array electrodes for sodium microbatteries. *Adv Funct Mater* **2018**;*28*:1704880.
145. Wang C, Zeng YX, Xiao X, Wu SJ, Zhong GB, Xu KQ, Wei ZF, Su W, Lu XH. Gamma-MnO_2 nanorods/graphene composite as efficient cathode for advanced rechargeable aqueous zinc-ion battery. *J Energy Chem* **2020**;*43*:182–7.
146. Guo RT, Ni LS, Zhang H, Gao X, Momen R, Massoudi A, Zou GQ, Hou HS, Ji XB. MnO_2 nanowires anchored with graphene quantum dots for stable aqueous zinc-ion batteries. *ACS Appl Energy Mater* **2021**;*4*:10940–7.
147. Long J, Yang ZH, Yang FH, Cuan J, Wu JX. Electrospun core-shell Mn_3O_4 /carbon fibers as high-performance cathode materials for aqueous zinc-ion batteries. *Electrochim Acta* **2020**. https://doi.org/10.1016/j.electacta.2020.136155 .
148. Xu CJ, Li BH, Du HD, Kang FY. Energetic zinc ion chemistry: the rechargeable zinc ion battery. *Angew Chem Int Ed* **2012**;*51*:933–5.
149. Zhang N, Cheng FY, Liu YC, Zhao Q, Lei KX, Chen CC, Liu XS, Chen J. Cation-deficient spinel $ZnMn_2O_4$ cathode in $Zn(CF_3SO_3)_2$ electrolyte for rechargeable aqueous Zn-ion battery. *J Am Chem Soc* **2016**;*138*:12894–901.
150. Tang F, He T, Zhang HH, Wu XW, Li YK, Long FN, Xiang YH, Zhu L, Wu JH, Wu XM. The MnO@N-doped carbon composite derived from electrospinning as cathode material for aqueous zinc ion battery. *J Electroanal Chem* **2020**;*873*:114368.
151. Huang JH, Wang Z, Hou MY, Dong XL, Liu Y, Wang YG, Xia YY. Polyaniline-intercalated manganese dioxide nanolayers as a high-performance cathode material for an aqueous zinc-ion battery. *Nat Commun* **2018**;*9*:2906.
152. Dong LB, Ma XP, Li Y, Zhao L, Liu WB, Cheng JY, Xu CJ, Li BH, Yang QH, Kang FY. Extremely safe, high-rate and ultralong-life zinc-ion hybrid supercapacitors. *Energy Stor Mater* **2018**;*13*:96–102.
153. Wang ZF, Ruan ZH, Liu ZX, Wang YK, Tang ZJ, Li HF, Zhu MS, Hung TF, Liu J, Shi ZC, Zhi CY. A flexible rechargeable zinc-ion wire-shaped battery with shape memory function. *J Mater Chem A* **2018**;*6*:8549–57.

154. Yu X, Fu YP, Cai X, Kafafy H, Wu HW, Peng M, Hou SC, Lv ZB, Ye SY, Zou DC. Flexible fiber-type zinc-carbon battery based on carbon fiber electrodes. *Nano Energy* **2013**;*2*:1242–8.
155. Zeng YX, Zhang XY, Meng Y, Yu MH, Yi JN, Wu YQ, Lu XH, Tong YX. Achieving ultrahigh energy density and long durability in a flexible rechargeable quasi-solid-state Zn-MnO_2 battery. *Adv Mater* **2017**;*29*:1700274.
156. Jian Z, Yang NJ, Vogel M, Leith S, Schulte A, Schonherr H, Jiao TP, Zhang WJ, Muller J, Butz B, Jiang X. Flexible diamond fibers for high-energy-density zinc-ion supercapacitors. *Adv Energy Mater* **2020**;*10*:2002202.
157. Liu Y, Wang J, Zeng YX, Liu J, Liu XQ, Lu XH. Interfacial engineering coupled valence tuning of MoO_3 cathode for high-capacity and high-rate fiber-shaped zinc-ion batteries. *Small* **2020**;*16*:1907458.
158. Wang CF, He T, Cheng JL, Guan Q, Wang B. Bioinspired interface design of sewable, weavable, and washable fiber zinc batteries for wearable power textiles. *Adv Funct Mater* **2020**;*30*:2004430.
159. Sun T, Li ZJ, Zhi YF, Huang YJ, Fan HJ, Zhang QC. Poly(2,5-dihydroxy-1,4-benzoquinonyl sulfide) as an efficient cathode for high-performance aqueous zinc-organic batteries. *Adv Funct Mater* **2021**;*31*:2010049.
160. Ma XM, Cao XX, Yao ML, Shan LT, Shi XD, Fang GZ, Pan AQ, Lu BA, Zhou J, Liang SQ. Organic-inorganic hybrid cathode with dual energy-storage mechanism for ultrahigh-rate and ultralong-life aqueous zinc-ion batteries. *Adv Mater* **2022**;*34*:2105452.
161. Zhang XG. Fibrous zinc anodes for high power batteries. *J Power Sources* **2006**;*163*:591–7.
162. Huy VPH, Hieu LT, Hur J. Zn metal anodes for Zn-ion batteries in mild aqueous electrolytes: challenges and strategies. *Nanomaterials* **2021**;*11*:2746.
163. Chao DL, Zhu C, Song M, Liang P, Zhang X, Tiep NH, Zhao HF, Wang J, Wang RM, Zhang H, Fan HJ. A high-rate and stable quasi-solid-state zinc-ion battery with novel 2D layered zinc orthovanadate array. *Adv Mater* **2018**;*30*:1803181.
164. Wang LP, Li NW, Wang TS, Yin YX, Guo YG, Wang CR. Conductive graphite fiber as a stable host for zinc metal anodes. *Electrochim Acta* **2017**;*244*:172–7.
165. Li HF, Yang Q, Mo FN, Liang GJ, Liu ZX, Tang ZJ, Ma LT, Liu J, Shi ZC, Zhi CY. MoS_2 nanosheets with expanded interlayer spacing for rechargeable aqueous Zn-ion batteries. *Energy Stor Mater* **2019**;*19*:94–101.
166. Zhang Y, Deng SJ, Pan GX, Zhang HH, Liu B, Wang XL, Zheng XH, Liu Q, Wang XL, Xia XH, Tu JP. Introducing oxygen defects into phosphate ions intercalated manganese dioxide/vertical multilayer graphene arrays to boost flexible zinc ion storage. *Small Methods* **2020**;*4*:1900828.
167. Wang DH, Li HF, Liu ZX, Tang ZJ, Liang GJ, Mo FN, Yang Q, Ma LT, Zhi CY. A nanofibrillated cellulose/polyacrylamide electrolyte-based flexible and sewable high-performance Zn-MnO_2 battery with superior shear resistance. *Small* **2018**;*14*:1803978.
168. Qiu WD, Li Y, You A, Zhang ZM, Li GF, Lu XH, Tong YX. High-performance flexible quasi-solid-state Zn-MnO_2 battery based on MnO_2 nanorod arrays coated 3D porous nitrogen-doped carbon cloth. *J Mater Chem A* **2017**;*5*:14838–46.
169. Zeng YX, Zhang XY, Qin RF, Liu XQ, Fang PP, Zheng DZ, Tong YX, Lu XH. Dendrite-free zinc deposition induced by multifunctional CNT frameworks for stable flexible Zn-ion batteries. *Adv Mater* **2019**;*31*:1903675.
170. Wang N, Zhai SL, Ma YY, Tan XH, Jiang KR, Zhong WB, Zhang WY, Chen N, Chen WF, Li SD, Han GY, Li Z. Tridentate citrate chelation towards stable fiber zinc-polypyrrole battery with hybrid mechanism. *Energy Stor Mater* **2021**;*43*:585–94.
171. Yang XZ, Li WP, Lv JZ, Sun GJ, Shi ZX, Su YW, Lian XY, Shao YY, Zhi AM, Tian XZ, Bai XD, Liu ZF, Sun JY. In situ separator modification via CVD-derived N-doped carbon for highly reversible Zn metal anodes. *Nano Res* **2021**. https://doi.org/10.1007/s12274-021-3957-z .
172. Cao J, Zhang DD, Zhang XY, Sawangphruk M, Qin JQ, Liu RP. A universal and facile approach to suppress dendrite formation for a Zn and Li metal anode. *J Mater Chem A* **2020**;*8*:9331–44.
173. Li C, Sun ZT, Yang T, Yu LH, Wei N, Tian ZN, Cai JS, Lv JZ, Shao YL, Rummeli MH, Sun JY, Liu ZF. Directly grown vertical graphene carpets as janus separators toward stabilized Zn metal anodes. *Adv Mater* **2020**;*32*:2003425.
174. Wang AR, Zhou WJ, Chen MF, Huang AX, Tian QH, Xu XW, Chen JZ. Integrated design of aqueous zinc-ion batteries based on dendrite-free zinc microspheres/carbon nanotubes/nanocellulose composite film anode. *J Colloid Interface Sci* **2021**;*594*:389–97.
175. Foroozan T, Yurkiv V, Sharifi-Asl S, Rojaee R, Mashayek F, Shahbazian-Yassar R. Non-dendritic Zn electrodeposition enabled by zincophilic graphene substrates. *ACS Appl Mater Interfaces* **2019**;*11*:44077–89.
176. Yang Y, Chen T, Yu B, Zhu M, Meng F, Shi W, Zhang M, Qi Z, Zeng K, Xue J. Manipulating Zn-ion flux by two-dimensional porous g-C_3N_4 nanosheets for dendrite-free zinc metal anode. *Chem Eng J* **2022**;*433*:134077.
177. Fang Y, Xie XS, Zhang BY, Chai YZ, Lu BA, Liu MK, Zhou J, Liang SQ. Regulating zinc deposition behaviors by the conditioner of PAN separator for zinc-ion batteries. *Adv Funct Mater* **2021**;*32*:2109671.
178. Yuan ZZ, Liu XQ, Xu WB, Duan YQ, Zhang HM, Li XF. Negatively charged nanoporous membrane for a dendrite-free alkaline zinc-based flow battery with long cycle life. *Nat Commun* **2018**;*9*:3731.
179. Zhang C, Shen L, Shen JQ, Liu F, Chen G, Tao R, Ma SX, Peng YT, Lu YF. Anion-sorbent composite separators for high-rate lithium-ion batteries. *Adv Mater* **2019**;*31*:1808338.
180. Huang ZM, Zhang YZ, Kotaki M, Ramakrishna S. A review on polymer nanofibers by electrospinning and their applications in nanocomposites. *Compos Sci Technol* **2003**;*63*:2223–53.

Publisher's Note Springer Nature remains neutral with regard to jurisdictional claims in published maps and institutional affiliations.

Springer Nature or its licensor holds exclusive rights to this article under a publishing agreement with the author(s) or other rightsholder(s); author self-archiving of the accepted manuscript version of this article is solely governed by the terms of such publishing agreement and applicable law.